DATA REGISTRATION AND FUSION FOR CARDIAC APPLICATIONS

Timo Mäkelä

Dissertation for the degree of Doctor of Science in Technology to be presented with due permission of the Department of Engineering Physics and Mathematics for public examination and debate in Auditorium F1 at Helsinki University of Technology (Espoo, Finland) on the 28th of May, 2003, at 12 o'clock noon.

Author   Timo Juhani Mäkelä

Name of the dissertation

Data registration and fusion for cardiac applications

Date of manuscript   January 27, 2003   Date of the dissertation   May 28, 2003

☐ Monograph   ☑ Article dissertation (summary + original articles)

Department	Department of Engineering Physics and Mathematics
Laboratory	Laboratory of Biomedical Engineering
Field of research	Medical image processing
Opponent	Prof. Nicholas Ayache (INRIA, Sophia Antipolis, France)
Supervisor	Prof. Toivo Katila (Helsinki University Of Technology)
Instructors	D.Sc. (Tech.) Outi Sipilä (HUCH), Dr. Isabelle Magnin and Dr. Patrick Clarysse (INSA Lyon)

Abstract

The registration and fusion of information from multiple cardiac image modalities such as magnetic resonance imaging (MRI), X-ray computed tomography (CT), positron emission tomography (PET) and single photon emission computed tomography (SPECT) has been of increasing interest to the medical community as tools for furthering physiological understanding and for diagnostic of ischemic heart diseases. Ischemic heart diseases and their consequence, myocardial infarct, are the leading cause of mortality in industrial countries. In cardiac image registration and data fusion, the combination of structural information from MR images and functional information from PET and SPECT is of special interest in the estimation of myocardial function and viability. Cardiac image registration is a more complex problem than brain image registration. The non-rigid motion of the heart and the thorax structures introduce additional difficulties in registration.

In this thesis the goal was develop methods for cardiac data registration and fusion. A rigid registration method was developed to register cardiac MR and PET images. The method was based on the registration of the segmented thorax structures from MR and PET transmission images. The thorax structures were segmented from images using deformable models. A MR short axis registration with PET emission image was also derived. The rigid registration method was evaluated using simulated images and clinical MR and PET images from ten patients with multivessel coronary artery diseases. Also an elastic registration method was developed to register intra-patient cardiac MR and PET images and inter-patient head MR images. In the elastic registration method, a combination of mutual information, gradient information and smoothness of transformation was used to guide the deformation of one image towards another image.

An approach for the creation of 3-D functional maps of the heart was also developed. An individualized anatomical heart model was extracted from the MR images. A rigid registration of anatomical MR images and PET metabolic images was carried out using surface based registration, and the registration of MR images with magnetocardiography (MCG) data using external markers.The method resulted in a 3-D anatomical and functional model of the heart that included structural information from the MRI and functional information from the PET and MCG. Different error sources in the registration method of the MR images and MCG data was also evaluated in this thesis. The results of the rigid MR-PET registration method were also used in the comparison of multimodality MR imaging methods to PET.

Keywords	medical image processing, cardiac image registration, data fusion, MR, PET, MCG, visualization	
UDC	616.12:616-073:004.92	Number of pages 108
ISBN (printed) 951-22-6514-1		ISBN (pdf) 951-22-6515-X
Publisher Helsinki University of Technology, Laboratory of Biomedical Engineering		
Print distribution		
☑ The dissertation can be read at http://lib.hut.fi/Diss/2003/isbn951226515X/		

Preface

The work for this thesis was carried out within the image processing group at the Laboratory of Biomedical Engineering, Helsinki University of Technology and at the CREATIS laboratory of INSA of Lyon, France. The work was carried out as a part of the graduate school "Functional Imaging in Medicine", the Academy of Finland's centre of excellence "Helsinki Brain Research Center" (HBRC) and as a part of several National Technology Agency of Finland (TEKES) funded projects.

I wish to thank Professor Toivo Katila, the supervisor of this thesis, for all the discussions and for providing excellent research enviroment for this work. I also wish to thank Dr. Isabelle Magnin, the head of the CREATIS laboratory of INSA Lyon, for support and excellent working conditions during my staying in Lyon. I would also like to thank my instructors D.Sc. (Tech.) Outi Sipilä and Dr. Patrick Clarysse for the research ideas and valuable guidance.

I would like to thank the preliminary examiners, Docent Ulla Ruotsalainen and Professor Philippe Cinquin for their corrections and suggestions for improving this thesis. Many thanks are also due to Docent Jyrki Lötjönen, Docent Jukka Nenonen, M.D. Kirsi Lauerma and D.Sc. (Tech.) Eero Salli for their many contributions and help to this work. Also Dr. Quoc Cuong Pham and M.Sc. Nicoleta Pauna from INSA Lyon own my gratitude for their many contributions and help to this work.

The people at the Laboratory of Biomedical Engineering, especially the former and current members of the image processing group, deserve my thanks for their assistance and for providing an inspiring atmosphere. Also the people at the CREATIS laboratory of INSA Lyon deserve my thanks for their assistance and friendliness during my totally over one year period in Lyon.

The financial support provided by the Finnish Cultural Foundation, The Jenny and Antti Wihuri Foundation, The Foundation of Technology in Finland, The Research Foundation of Helsinki University of Technology, the scientific Department of the French Embassy in Finland and the Region Rhône Alpes, through the ADéMO project is gratefully acknowledged.

Finally, I want to express my gratitude to my parents, relatives and friends for their support. Last, but certainly not least, I thank to my wife Ulla for her support and with her also our son Mikael (2 months) of the patience during the preparation of this work.

Espoo, May 2003

Timo Mäkelä

Contents

List of publications

This thesis consists of an overview and of the following six publications:

I T.J. Mäkelä, P. Clarysse, O. Sipilä, N. Pauna, Q.C. Pham, T. Katila and I.E. Magnin (2002). A review of cardiac image registration methods. *IEEE Trans. Med. Imaging* 21:1011-1021.

II T.J. Mäkelä, P. Clarysse, J. Lötjönen, O. Sipilä, K. Lauerma, H. Hänninen, E.-P. Pyökkimies, J. Nenonen, J. Knuuti, T. Katila and I.E. Magnin (2001). A new method for the registration of cardiac PET and MR images using deformable model based segmentation of the main thorax structures. In *Proc. of the 4nd International conference on Medical Image Computing and Computer Assisted Intervention (MICCAI'01)*. W. Niessen, M.A. Viergever (Eds.). Springer. *Lect. Notes Comput. Sci.* 2208:557-564.

III T.J. Mäkelä, Q.C. Pham, P. Clarysse, J. Nenonen, J. Lötjönen, O. Sipilä, H. Hänninen, K. Lauerma, J. Knuuti, T. Katila and I.E. Magnin. A 3-D model-based registration approach for the PET, MR and MCG cardiac data fusion. *Medical Image Analysis*, accepted for publication.

IV J. Lötjönen and T.J. Mäkelä (2001). Elastic matching using a deformation sphere. In *Proc. of the 4nd International conference on Medical Image Computing and Computer Assisted Intervention (MICCAI'01)*. W. Niessen, M.A. Viergever (Eds.). Springer. *Lect. Notes Comput. Sci.* 2208:541-548.

V T.J. Mäkelä, J. Lötjönen, O. Sipilä, K. Lauerma, J. Nenonen, T. Katila and I.E. Magnin (2002). Error analysis of registering of anatomical and functional cardiac data using external markers. In *Proc. 13th Int. Conf. on Biomagnetism (BIOMAG'02)*. H. Nowak, J. Haueisen, F. Giesler, R. Huonker (Eds.). Verlag. Pages 842-845.

VI K. Lauerma, P. Niemi, H. Hänninen, T. Janatuinen, L-M. Voipio-Pulkki, J. Knuuti, L. Toivonen, T.J. Mäkelä, M. Mäkijärvi and H.J. Aronen (2000). Multimodality MR imaging assessment of myocardial viability: combination of first-pass and late contrast enhancement to wall motion dynamics and comparison with FDG PET – initial experience. *Radiology* 217:729-736.

Throughout the overview these publications are referred by their Roman numerals.

List of abbreviations and symbols

2-D	two-dimensional
3-D	three-dimensional
4-D	four-dimensional
BSPM	body surface potential mapping
CDE	current density estimates
CR	correlation ratio
CT	X-ray computed tomography
ECG	electrocardiography
FDG	2-[fluorine 18]fluoro-2-deoxy-D-glucose
HUCH	Helsinki University Central Hospital
LA	long axis
LV	left ventricle
MAP	maximum a posteriori
MCG	magnetocardiography
MRI	magnetic resonance imaging
NMI	normalized mutual information
NMR	nuclear magnetic resonance
PET	positron emission tomography
RMS	root mean square
RV	right ventricle
SA	short axis
SORTEO	Simulator of Realistic Tridimensional Emitting Objects
SPECT	single photon emission computed tomography
SQUID	superconducting magnetometer
SDV	standard deviation
T	Tesla
US	ultrasonography
VTK	Visualization Toolkit Software

1   Introduction

The integration of data from different medical imaging modalities is often desired for diagnostic purposes and in cardiac research. A first step in this integration process is to bring modalities involved into a spatial alignment, a procedure referred to as *registration* (Maintz and Viergever, 1998). After registration, a fusion step is required to visualize the integrated information from the data involved.

In this thesis the main interest was to develop methods to combine information from different cardiac data modalities. In cardiac image registration and data fusion, the integration of multiple complementary information into a common reference allows a more comprehensive analysis of cardiac functions and pathologies. Specifically, the interest in multimodality cardiac image registration and data fusion lies in the determination and quantification of the viable tissues in ischemic heart diseases. A viable tissue is a pathological tissue that can recover after a blood-flow re-establishment. The quantification of the viability can help to decide whether or not a patient with coronary artery disease will benefit from a revascularization procedure. Viability estimation, together with ischemic diagnosis, both rely on the joint analysis of the perfusion, metabolism, and contractile function, with each of these being quantified with specific imaging modalities (Fig. 1).
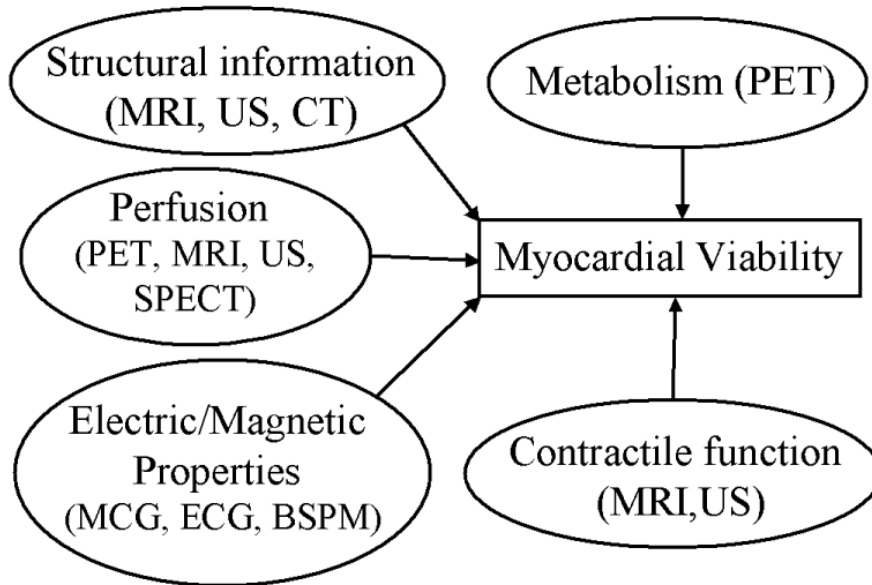
Figure 1: Cardiac data registration and fusion for viability studies (Publ. III).

The registration and fusion of structural and functional information from medical images is of special interest to the medical community. Structural information from the heart can be obtained by using magnetic resonance imaging (MRI), X-ray computed tomography (CT) and ultrasonography (US). Functional information can be obtained by analyzing the metabolism with positron emission tomography (PET), perfusion with thallium single photon emission computed tomography (SPECT), MRI, US or PET, and contractile function by using MRI and US. The functional electrical activity of the heart creates both an electric and a magnetic fields and these can be measured by using electrocardiography (ECG) and magnetocardiography (MCG), respectively (Siltanen, 1988). ECG, MCG and multichannel ECG mapping techniques, such as body surface potential mapping (BSPM) (Ambroggi et al., 1989; Simelius, 1998), give unique additional information on the electromagnetic manifestations of myocardial ischemia and viability.

In this thesis, MRI, PET and MCG cardiac data modalities were utilized. MRI (Lauterbur, 1973) is based on the principles of the nuclear magnetic resonance (NMR). In clinical applications, the NMR signal from the hydrogen nuclei is normally used for imaging (Webb, 1995). In cardiac MR studies short axis (SA) and long axis (LA) images are usually acquired. Scout images are first used to define the heart LA and SA orientations. After that SA cardiac cine images consisting of several slices from the valve level down to the apex can be acquired. ECG-gating and breath holding are commonly used in order to improve image acquisition quality and to reduce registration errors caused by cardiac movement and respiration. Some of the advantages of MR imaging are that it is non-invasive, it provides free selection of the imaging plane and provides good contrast between different soft tissue types (Conolly et al., 1995). Tagged MRI is an accurate technique for heart wall deformation analysis (Kerwin, 2000). Heart wall motion abnormalities are sensitive indicators of disturbed myocardial blood flow (Ratib, 2000). The development of faster MR imaging sequences has also made it possible to determine the first pass circulation of the contrast bolus using MRI, which also enables myocardial perfusion studies (Hartiala and Knuuti, 1995). Compared with US, MR imaging is more accurate for the viability assessment because MR images can be acquired with reproducible quality that is independent of the examiner or the patient's anatomy (Baer et al., 1996).

PET imaging (Sweet, 1951; Wrenn and Handlerp, 1951; Brownell and Sweet, 1953) can provide information about the perfusion and the metabolic activity of the heart (Budinger and VanBrockling, 1995). PET has been used to assess the benefit of coronary artery bypass surgery and in viability studies (Hartiala and Knuuti, 1995). The 2-[fluorine 18]fluoro-2-deoxy-D-glucose (FDG) PET imaging provides information on the glucose metabolism of the heart. This method is considered to be the gold standard in determining viable areas of the heart (Hartiala and Knuuti, 1995). PET enables to quantify the regional myocardial perfusion in absolute terms. In PET acquisitions, the images are usually static, i.e., presents integrated information over time. However, with modern scanners, it is also possible to acquire ECG-gated images. With dynamic acquisitions, the time course of the radiotracer uptake is followed in regions of interest (Gilardi et al., 1996). In addition to the functional PET emission images, PET transmission images are also acquired for attenuation correction of the emission image and are obtained using an external radioactive source (e.g., germanium-68). PET transmission images resembles a low quality CT image and it offers structural information that can be used for segmentation and registration purposes (Kim et al., 1991; Pallotta et al., 1995).

The MCG method allows a comprehensive study of the electromagnetic fields of the heart. In MCG, magnetic fields produced by the electrical activity of the heart are recorded noninvasively, by using superconducting magnetometers (SQUIDs) (Hämäläinen and Nenonen, 1999). Biomagnetic fields measured outside the body are extremely low in magnitude (10 fT to 100 pT). Measured signals are generated by the electrical currents in myocardial cells, and therefore the measurements provide direct real-time functional information about the heart (Hämäläinen and Nenonen, 1999). The time scale of the detectable signals ranges from fractions of a millisecond to several seconds, or even longer periods. The region of the source activity is calculated by using data obtained from the SQUID-sensors. In most cases the goal of the data-analysis is to solve the inverse problem, i.e., estimate the source current density underlying measured external fields (Nenonen, 1994). In other words, a current distribution that would yield the measurement result is calculated. A minimum-norm estimate is often used in estimating the primary current distribution but, because this inverse problem is ill-posed, regularization has to be applied (Nenonen, 1997). MCG is currently used at some hospitals to test and further develop its clinical use (Hämäläinen and Nenonen, 1999). Multichannel MCG studies are particularly promising in noninvasively locating abnormal cardiac activities critical for the arousal of arrhythmia (Nenonen, 1997).

In this thesis the goal was to develop methods for cardiac data registration and fusion which are of increasing interest in the medical community as tools for furthering physiologic understanding and for diagnostic of ischemic heart diseases (Publ. I). In particularly, the aim of this thesis was to develop methods to combine cardiac anatomical data from MRI and functional data of the metabolism from FDG PET and of the electromagnetic activity from MCG. Therefore, a new rigid registration method was developed to register cardiac MR and FDG PET images (Publ. II). The developed method is presented and evaluated in Section 3.2. The registration method of cardiac anatomical MR and functional MCG data and evaluation of different error sources in the registration method is described in Section 3.3 (Publ. III and V). Also a new elastic registration method was developed (Publ. IV) and it was applied e.g. to compensate for heart motion in intra-subject studies (Section 3.4). Last, the results of the rigid MR and FDG PET registrations were utilized in order to build a complete procedure for the 3-D patient-specific anatomic functional model of the heart (Publ. III). This is presented in Section 3.5. Section 3.6 contains applications for cardiac viability studies. Results are discussed in Chapter 4 followed by the general conclusions (Chapter 5). Chapter 6 sum up the publications after which author's contribution to different publications is detailed. This thesis consists of an overview, which also includes some new material, and of the six publications.

2   Registration methods for cardiac images

Several survey articles and books have been published in the field of medical image registration (Brown, 1992; Maurer and Fizpatrick, 1993; van den Elsen et al., 1993; Maintz and Viergever, 1998; Lester and Arridge, 1998; Fitzpatrick et al., 2000; Audette et al., 2000; Bankman, 2000; Hill et al., 2001; Frangi et al., 2001; Hajnal et al., 2001). Only a few review articles concentrate on cardiac image registration (Habboosh, 1992; Gilardi et al., 1996). Gilardi et al. (1996) presented a review of the techniques and clinical applications for the integration of multi-modal biomedical images of the heart and Habboosh (1992) briefly discussed aspects of cardiac PET and MRI registration. Also, in the review article by Maintz and Viergever (1998), the registration methods for cardiac images were referred to in a separate section. In Publication I, a review of cardiac image registration methods is presented, including the most recent articles, and implementation and validation issues are also discussed. Registration methods are usually composed of the following main components: a transformation that maps one image onto another, a similarity criterion, which indicates when one image mostly resemble another image and an optimization process which efficiently estimates the best transformation parameters. Evaluation of registration method is also evident and important issue that is often neglected.

2.1   Image transformations

Registration methods are classified into the rigid, affine, projective and curved or elastic methods depending on the nature of the registration transformation (Maintz and Viergever, 1998) (Fig. 2). A transformation is called *global* if applied to the whole image and *local* if applied to subsections of the image that each have their own transformation defined.
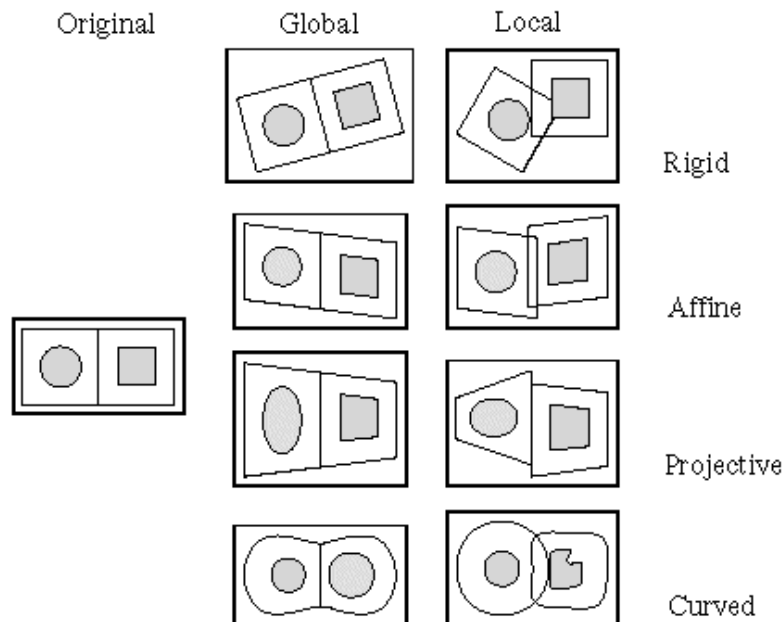
Figure 2: Transformations of 2-D images (Maintz and Viergever, 1998).

In global rigid registration only translations and rotations are allowed and the distances between points and angles between lines cannot change during registration (van den Elsen et al., 1993). Affine registration methods map parallel lines onto parallel lines, projective registration lines onto lines and curved or elastic registration method lines onto curves (Maintz and Viergever, 1998; Fitzpatrick et al., 2000).

2.2   Similarity criteria

Methods for cardiac and thorax image registration can be divided into two main categories: (1) registration methods based on geometric image features and (2) methods based on voxel similarity measures (Publ. I).

The geometric image feature based methods can be divided into registration of *a set of points* and methods which register *edges or surfaces*. Cardiac image registration methods are often validated using phantom experiments where a corresponding sets of external marker points are registered (Pallotta et al., 1995; Yu et al., 1995; Eberl et al., 1996; Gilardi et al., 1998; Dey et al., 1999). Also, landmark based validations typically uses a registration of sets of the corresponding landmark points (Kramer et al., 1989; Savi et al., 1995; Sinha et al., 1995; Eberl et al., 1996; Gilardi et al., 1998; Carrillo et al., 2001; Bidaut and Vallée, 2001). Landmarks have also been utilized for the elastic registration of the thorax MR image to the coordinates of a CT image (Wirth et al., 1997). In Publication V a skin marker based registration method was used to register cardiac MR images and MCG data. A non-iterative least-squares method (Arun et al., 1987) was used to register point sets of the corresponding markers. *Edge and surface* based cardiac and thorax registration methods include methods which register heart surfaces (Faber et al., 1991; Thirion, 1995; Sinha et al., 1995; Andersson et al., 1995; Declerck et al., 1997; Thirion, 2001; Nekolla et al., 2000) and thorax surfaces (Pallotta et al. (1995); Yu et al. (1995); Tai et al. (1997); Gilardi et al. (1998); Cai et al. (1999), Publ. II). In registration methods in which a transmission image (PET, SPECT) is used as an linking mediator to register corresponding emission image, the assumption is that patient does not move during and between transmission and emission image acquisition (Kim et al. (1991); Pallotta et al. (1995); Yu et al. (1995); Tai et al. (1997); Gilardi et al. (1998); Cai et al. (1999), Publ. II). Because the image acquisition times in cardiac PET and SPECT transmission and emission images are often several minutes, movement artifacts often occurs. For SPECT imaging it has been presented that if the movement between cardiac SPECT transmission and the emission image is more than 2-3 cm, it can also seriously affect the attenuation correction of the emission image and, thus, its quality (Stone et al., 1998).

In Publication II a thorax surface based registration method for cardiac MR and FDG PET images was presented. The method differed from the previously introduced thorax surface based registration methods (e.g. Pallotta et al. (1995); Gilardi et al. (1998)), especially as it performed an automatic deformable model based segmentation of the thorax and lung surfaces from both PET transmission and thorax MR images. Another advantage of the developed registration method was that it not only provided registered transaxial images but that it also provided registered SA images of the heart.

Registration methods based on voxel similarity measures include *moments and principal-axes methods*, *intensity difference and correlation methods* and methods based on *mutual information*. The *moments and principal-axes methods* have been mainly used in the initialization steps of other, more accurate methods (Slomka et al., 1995; Dey et al., 1999). The *intensity difference* methods have been mainly used for intramodality registrations (Hoh et al., 1993; Slomka et al., 1995, 2001b; Bidaut and Vallée, 2001; Klein et al., 2002; Klein and Huesman, 2002) and also in few cases for intermodality registrations (Eberl et al., 1996; Dey et al., 1999). Further, *correlation methods* have been mainly used for intramodality registrations (Bettinardi et al., 1993; Bacharach et al., 1993; Turkington et al., 1997; O'Connor et al., 1998; O'Connor, 2000; Gallippi and Trahey, 2001) and also for intermodality registration of segmented thorax structures (Kim et al., 1991). Cardiac and thorax image registration methods based on *mutual information* are not very numerous in the literature at the moment (Slomka et al. (2000); Carrillo et al. (2001); Slomka et al. (2001a); Zhenghong and Berridge (2002); McLeish et al.

(2003); Shekhar and Zagrodsky (2002); Mattes et al. (2003), Publ. IV, Mäkelä et al. (2003)). In Publication IV an elastic cardiac MR-PET image registration method was developed which combined mutual information, gradient information and smoothness of the transformation to guide the deformation of one image towards another image.

Manual methods (Waiter et al., 2000; Behloul et al., 2001) can be considered to be a separate category of registration methods. They usually rely on an expert's ability to interactively register images. Images are often been interpolated to the same voxel dimensions before manual registration.

2.3   Registration principles

Several types of registration methods have been used to perform the registration. The choice of a cardiac image registration method is difficult since, at the present time, no general fully automatic method exist which could handle the wide variety of the encountered clinical situations (modalities, acquisition protocols etc.).

Methods based on geometric features

The chamfer matching method (Borgefors, 1986, 1988) is often used to register surfaces and point sets. In this method the sum of the distances between the transformed points and a distance map built upon the segmented surfaces using the chamfer distance transformation is minimized (Herk, 2000). For cardiac image registration, chamfer matching methods have mainly been utilized for registration methods based on the thorax structures (Pallotta et al. (1995); Gilardi et al. (1998); Cai et al. (1999), Publ. II). Also, the ICP algorithm of Besl and McKay (1992) has been used to register lines and surfaces (Declerck et al., 1996, 1997). In the ICP algorithm, the distances between structures are explicitly computed at every iteration of the registration and the sum of distances is minimized. The "head-and-hat" algorithm (Pelizzari et al., 1989; Levin et al., 1988) has also commonly been used to register medical images and was first used to register brain images. The algorithm models the contours from one image (usually higher resolution image) as a surface (the "head") and the contours of the other image as a series of points (the "hat"). The "head-and-hat" method determines the optimum for the transformation, which minimizes the mean squared deviation between the points of the "hat" and the surfaces of the "head" by using Powell's algorithm for minimization. The method has been applied in the registration of cardiac (Faber et al., 1991; Sinha et al., 1995) and thorax images (Yu et al., 1995).

Methods based on voxel similarity measures

The principle of the registrations methods using voxel similarity based measures relies on the iterative transformations of the source image to map to the target image at convergence (Maes et al., 1997; Hajnal et al., 2001; Woods, 2000a). These approaches requires the evaluation of the transformation each time a new set of the transformation parameters is selected. The speed of a registration algorithm depends on factors such as the need of the preprocessing, the complexity of the cost function and the number of the cost function evaluations performed by the optimization algorithm (Herk, 2000). With voxel similarity based registration methods the number of the cost function evaluations is usually high. Fast cost function evaluation techniques and multi-resolution schemes are likely to speed up the convergence of these kind of registration algorithms (Slomka et al. (2001a), Publ. IV).

2.4   Obtaining optimal transformation

For the optimization of a rigid 3-D image registration a cost function of 6 parameters (3 translations and 3 rotations) is normally minimized. In affine, projective and curved or elastic registration methods cost function has more parameters than with rigid registration. A global search to find the minimum (or maximum) of the cost function is usually computationally too heavy and time consuming. Optimization methods aim at find the optimum faster than more exhaustive global search. Methods that do not require the evaluation of the gradient of the cost function are usually privileged. Therefore, the Powell optimization method (Powell, 1962; Press et al., 1992) has been widely used in cardiac and thorax registration methods (Faber et al., 1991; Yu et al., 1995; Cai et al., 1999; Dey et al., 1999; Carrillo et al., 2001; Slomka et al., 2000, 2001a) as well as the Simplex optimization method (Nelder and Mead, 1965; Press et al., 1992) for cardiac image registration (Hoh et al., 1993; Slomka et al., 1995; Eberl et al., 1996; Dey et al., 1999; Slomka et al., 2001b). Also, multi-resolution methods can be advantageously adopted to increase the probability of finding the global optimum in the parameter space and to make the registration procedure faster (Pallotta et al. (1995); Bidaut and Vallée (2001); Slomka et al. (2001a), Publ. IV).

2.5   Evaluation of the registration

Evaluation of the registration accuracy is a difficult task in medical imaging because the ground truth (i.e., the gold standard) is generally not available (Fitzpatrick et al., 2000; Woods, 2000b; Hajnal et al., 2001). Evaluation of registration methods is often performed using external markers or anatomical landmarks as gold standards (Woods, 2000b). Visual inspection is the most obvious method for the qualitative evaluation of the registration accuracy but it is considered as an informal and insufficient approach. For registration methods based on thorax surfaces, registration accuracy has been evaluated using thorax phantoms (Bettinardi et al., 1993; Pallotta et al., 1995; Yu et al., 1995; Eberl et al., 1996; Gilardi et al., 1998; Kramer et al., 1989; Cai et al., 1999; Dey et al., 1999) or a heart phantom (Turkington et al., 1997). Klein *et al.* (Klein et al., 2002; Klein and Huesman, 2002) utilized a mathematical cardiac phantom (Pretorius et al., 1997) to evaluate a 4-D motion correction algorithm of cardiac PET images. Simulated images can also be used to estimate cardiac image registration accuracy (Pallotta et al., 1995; Tai et al., 1997; Pauna et al., 2003; Mäkelä et al., 2003). Integrated imaging devices such as combined PET/CT scanners (Beyer et al., 1999; Patton et al., 2000) could also provide gold standards for registration (Goerres et al., 2002). Principal cardiac image registration methods and their main parameters, including information on accuracy, are summarized in Table I.

Table 1: OVERVIEW OF EVALUATED CARDIAC AND THORAX IMAGE REGISTRATION METHODS (Publ. I)

Reference	Modalities	Object	Trans.	Struc.	Method	Valid.	Error	Error type
Registration methods based on geometric image features								
Point-based registration								
Wirth et al. (1997)	CT-MR	Thorax	Elastic	LM	int. & elast.	-	-	-
Thorax surface based registration								
Yu et al. (1995)	CT-PET	Thorax	Rigid	T&L	h&h	P	(x,y) 2.3 mm, (y) 3.0 mm	mean (RMS)
Cai et al. (1999)	CT-PET	Lungs	Rigid	T&L	CM	P& Pa.&SU	(x,y) 2-3 mm, (y) 3 - 4 mm, (rot.)1.5°	mean
Pallotta et al. (1995)	PET-PET	Heart	Rigid	T&L	CM	P&SI	3 mm, (rot.) 1 °	mean (RMS)
							2.19 ± 0.52 mm	mean(RMS)± SDV
Gilardi et al. (1998)	SPECT-PET	Heart	Rigid	T&L	CM	P&Pa.	(x,y) 3 mm, 5 mm (z)	(x,y)mean (RMS), (z)mean
Publication II	MR-PET	Heart	Rigid	T&L	CM	SU	(x,y,z) 2.8 ± 0.5 mm	mean±SDV
Mäkelä et al. (2003)	MR-PET	Heart	Rigid	T&L	CM	SI	(x,y,z) 8.2 ± 2.3 mm	mean±SDV (RMS)
Heart surface based registration								
Faber et al. (1991)	MR-SPECT	Heart	Rigid	HS	h&h	P	2.7 mm	mean (RMS)
Sinha et al. (1995)	MR-PET	Heart	Rigid	HS	h&h	LM	1.95 mm ± 1.6 mm	mean (RMS)
Nekolla et al. (2000)	PET-SPECT	Heart	Rigid	HS	-	SU	2.5 mm	mean
Registration methods based on voxel similarity measures								
Intensity difference and correlation methods								
Gallippi et al.(2001)	MR-MR (time series)	Heart	Rigid & Elastic	-	C	M	1.23 ± 0.06 mm / 3.25 ± 1.04 mm	left-right(mean) / ant.-post.(mean)
Bidaut et al. (2001)	MR-MR (perfusion)	Heart	Rigid	-	SSD	LM	3.0 mm (x), 1.6 mm (y), 2.2 mm (z)	mean (RMS) (maximum)
Bacharach et al. (1993)	PET-PET	Heart	Rigid	-	CC	M	(x,y,z) 1 mm, (rot.) 1.5 °	mean
Turkington et al. (1997)	PET-PET	Heart	Rigid	-	C	P	(x,y) 1.7 mm, (z) 4.2 mm	mean
Klein et al. (2002)	PET-PET	Heart	Elastic (4-D)	-	LS	P	(x) 1.9 mm, (y) 2.4 mm, (z) 6.8 mm	mean (max.)
Hoh et al. (1993)	MR-SPECT	Heart	Rigid	-	SAD, SSC	M	(x,y) 0.5 ± 0.5 mm, (z) 1.1 ± 1.1 mm, (rot) 0.9 ± 1.1 °	mean ± SDV
Dey et al. (1999)	CT-SPECT	Heart& Thorax	Rigid	-	SAD / VIR	P / P	2.5 ± 1.2 mm / 3.3 ± 1.3 mm	mean (RMS) / mean (RMS)
Eberl et al. (1996)	SPECT-SPECT	Heart	Rigid	-	SAD	P	3.1 ± 1.7 mm 1.3 °(rot)	mean ± SDV
Slomka et al. (1995)	SPECT-SPECT	Heart	Affine	-	SAD	P	1.5 mm(x,y,z), 2.0° (rot), 5.3 % (size)	mean (max.)
Mutual information								
Carrillo et al. (2001)	MR-MR	Abdom.	Rigid	-	MI	LM	(x,y,z) 3.05 mm	mean
Mäkelä et al. (2003)	MR-PET	Heart	Rigid	-	NMI	SI	(x,y,z) 4.6 ± 1.4 mm	mean±SDV (RMS)

Keys to Table I.:
Object = *Main object to be registered.*
Trans. = *Transformation method* (rigid, elastic, affine).
Struc. = *Registered structures* (T=Thorax, L=Lungs, LM=Landmarks, HS=heart surfaces).
Method = *Method used in registration* (C = cross-correlation, CC = correlation coefficient, CM = chamfer matching, elast. = elastic mapping functions, h&h="head-and-hat", int. = interpolation, LS = least squares voxel difference, MI = mutual information, NMI = normalized mutual information, SAD = sum of absolute differences, SSC = stochastic sign change, SSD = sum of squared intensity difference, VIR = varianceof intensity ratio).
Valid. = *Validation method* (P = phantom, Pa. = patient, SI = simulated images, M = misaligned images, LM = landmarks, SU = surfaces).
Error: rot. = rotational error.

3   Developed methods

In this chapter, cardiac data registration and fusion methods developed in this thesis are presented. The cardiac data utilized in this work is introduced in Section 3.1. A developed rigid registration method for cardiac MR and FDG PET images is presented and evaluated in Section 3.2 (Publ. II), the method for registering cardiac MR images and MCG data is described in Section 3.3 (Publ. III and Publ. V) and the elastic registration method in Section 3.4 (Publ. IV). A 3-D model based approach for combining information from MR and FDG PET images and MCG data is presented in Section 3.5 (Publ. III), and Section 3.6 contains applications for cardiac viability studies.

3.1   Cardiac data in this work

In this work, MR and FDG PET transmission and emission data (Publications II, III, IV and VI) and MCG data (Publication III) were obtained from ten patients (E1 - E10, mean age was 69, 8 men, 2 women) suffering from multivessel coronary artery disease, diagnosed with coronary angiography and regional dyskinesia in cineangiograms (Publ. VI). All patients underwent MR imaging and FDG PET imaging within 10 days. After this they were treated by having coronary bypass surgery. Six months later the MRI was repeated for the assessment of the myocardial response to revascularization. In this work the preoperative MR images were used.

3.1.1   MRI data

MR data were acquired with a 1.5 T Siemens Magnetom Vision imager (Siemens, Erlangen, Germany) at the Department of Radiology in Helsinki University Central Hospital (HUCH). Usually two images were obtained: a transaxial ECG-gated thorax image, consisting of about 40 slices from the neck down to the pelvis, and a SA cardiac cine image consisting of 5 to 10 slices from the valve level down to the apex. Transaxial thorax images were acquired during free respiration using a TurboFLASH sequence (Siemens, 2001; Raichura et al., 2001) with a body array coil. The pixel sizes and the slice thickness for transaxial images were 1.95 x 1.95 mm^2 and 10 mm, respectively (Fig. 3a). The SA MR slices (Fig. 3b) consisted of 10 to 15 cardiac phases and were acquired using ECG-gating and breath-hold. The pixel sizes for the SA slices were 1.25 mm x 1.25 mm^2 and the slice thickness was 7 mm with 15 mm distance between slices. The MR data in Publication V was acquired using different parameters (see Publication V for details).
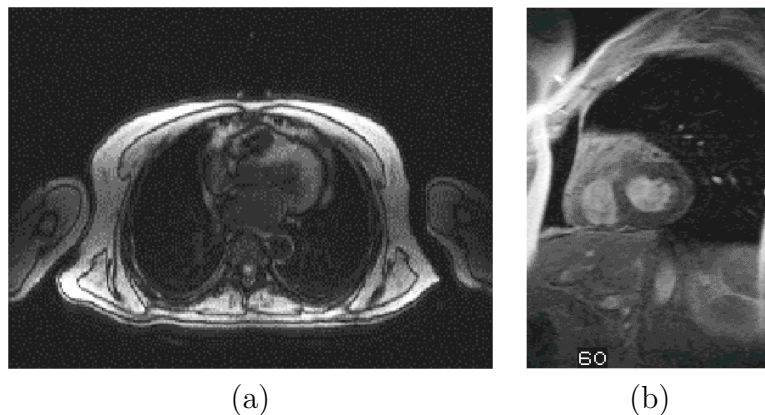

(a)   (b)

Figure 3: (a) Transaxial and (b) SA MR images (Publ. II, Publ. III).

A typical acquisition protocol with ECG-gated cardiac MRI is illustrated in Fig. 4. There is a spatio-temporal image acquisition problem while acquiring ECG-gated cardiac MR images: with sequences the same anatomical region is not observed within the frames at the same slice level. Between end-diastole and end-systole (during cardiac cycle) the heart valvular plane moves 9-14 mm towards the apex, and the myocardial walls thicken from approximately 10 mm to over 15 mm (Rogers et al., 1991; O'Dell et al., 1995; Klein and Huesman, 2002).
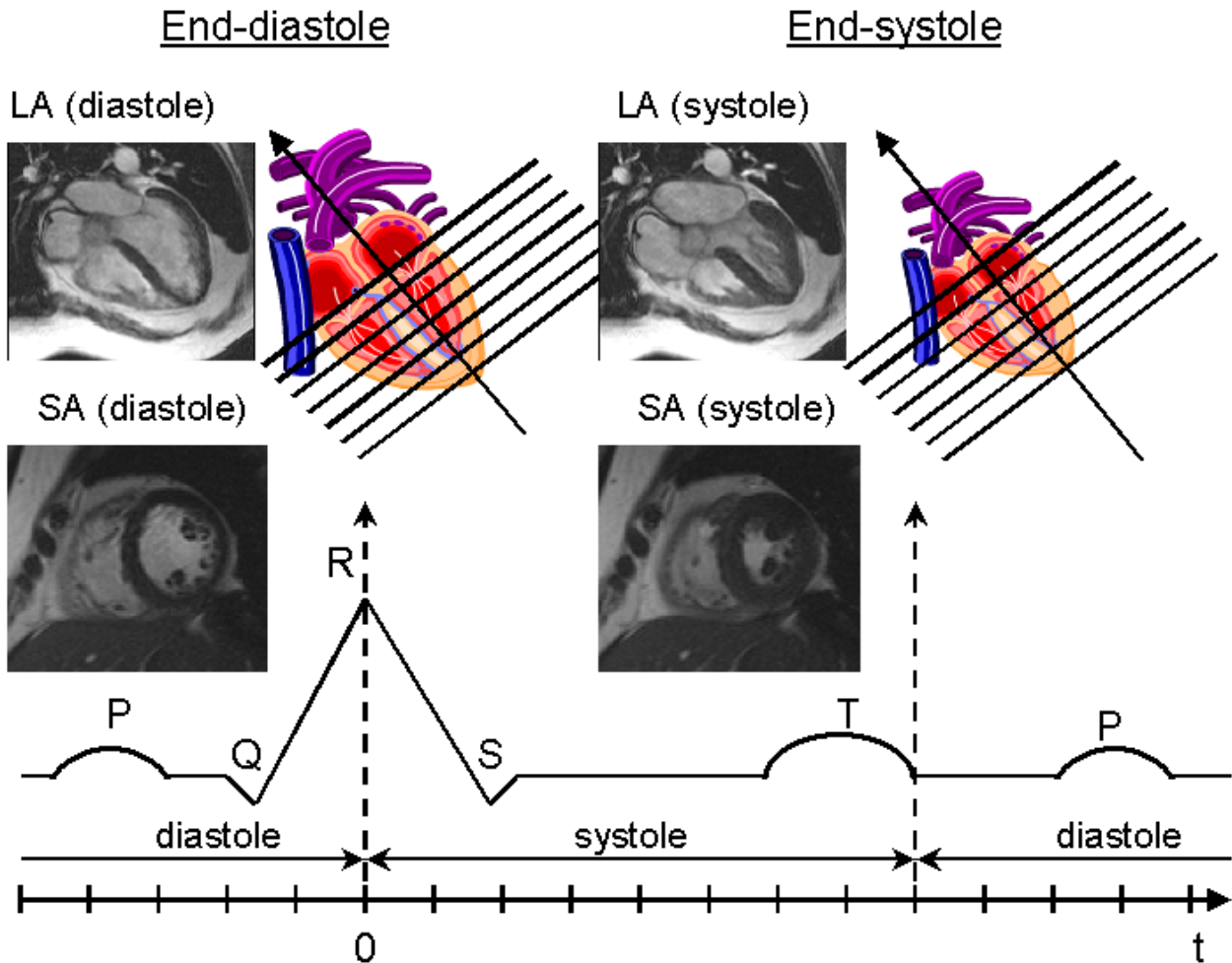

Figure 4: SA image acquisition with a ECG-gated cine MR sequence. MR SA and LA images (HUCH / Radiology) are presented at end-diastolic and end-systolic time points. Due to the 3-D motion of the heart we do not observe the same anatomical region within the same slice (Publ. I).

3.1.2   PET data

The static cardiac FDG PET and PET transmission data were acquired with a Siemens ECAT 931/08-12 (Siemens/CTI, Knoxville, USA) PET scanner at the Turku PET Centre. A series of 15 contiguous PET transmission and FDG PET emission images were obtained (Fig. 5a, 5b). For both transmission and emission images the pixel sizes and the slice thickness were 2.41 x 2.41 mm^2 and 6.75 mm, respectively.

PET transmission images were used for the attenuation correction of emission images but this also gave structural information that was utilized for registration purposes (Publ. II). The

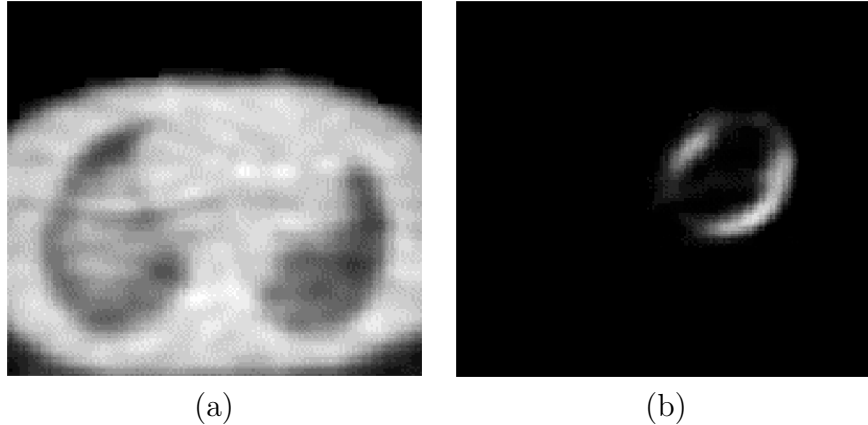(a)   (b)

Figure 5: (a) PET transmission and (b) FDG PET emission images (Publ. II).

FDG PET emission image gives information about the glucose metabolism in myocardial tissue. PET emission and transmission images were taken one after each other without moving the patient and if no serious movement artifacts happened between or during image acquisitions the FDG PET emission image can assumed to be registered with the corresponding transmission image (Kim et al., 1991; Bacharach et al., 1993; Bettinardi et al., 1993; Pallotta et al., 1995; Gilardi et al., 1996).

3.1.3   MCG data

The MCG measurements were performed at rest and after stress with a 67-channel cardio-magnetometer (4-D NeuroImaging, Helsinki, Finland) at the BioMag Laboratory at HUCH (Montonen et al., 2000). Acute ischemia was induced by exercise testing with a non-magnetic stress ergometer (Hänninen et al., 2001), pedaled in a supine position. The ST-segment difference signals of averaged post-stress and rest recordings were used in computing current density estimates (CDE) (Nenonen et al., 2001). In this work the depolarization (QRS complex) data at rest was utilized. Patient-specific boundary-element torso models were acquired from MR images, including the triangulated thorax and left ventricular (LV) surfaces (Lötjönen et al., 1999; Pham et al., 2001). The torso was assigned a constant electrical conductivity. Discrete CDE values were computed on the LV at midwall locations. A maximum a posteriori (MAP) estimator was used for the regularization of the inverse-problem (Nenonen et al., 2001).

3.2   Surface based registration method for cardiac MR and PET images

The rigid registration method for cardiac FDG PET and MR image registration is presented in Publication II. The method is based on registration of the thorax and lung surfaces, which are visible in both PET transmission and MR transaxial image. The main steps of the registration method are presented in Fig. 6 and described below:

1) Image resizing to get the same isotropic voxel dimensions for transaxial MR and PET transmission images and FDG PET emission images. Tri-linear interpolation was used to resize PET transmission and emission images in order to correspond to the isotropic MR image voxel size.

2) Automatic segmentation of the thorax and lungs was performed for the transaxial MR and PET transmission images using a method based on 3-D deformable models (Lötjönen et al., 1999).
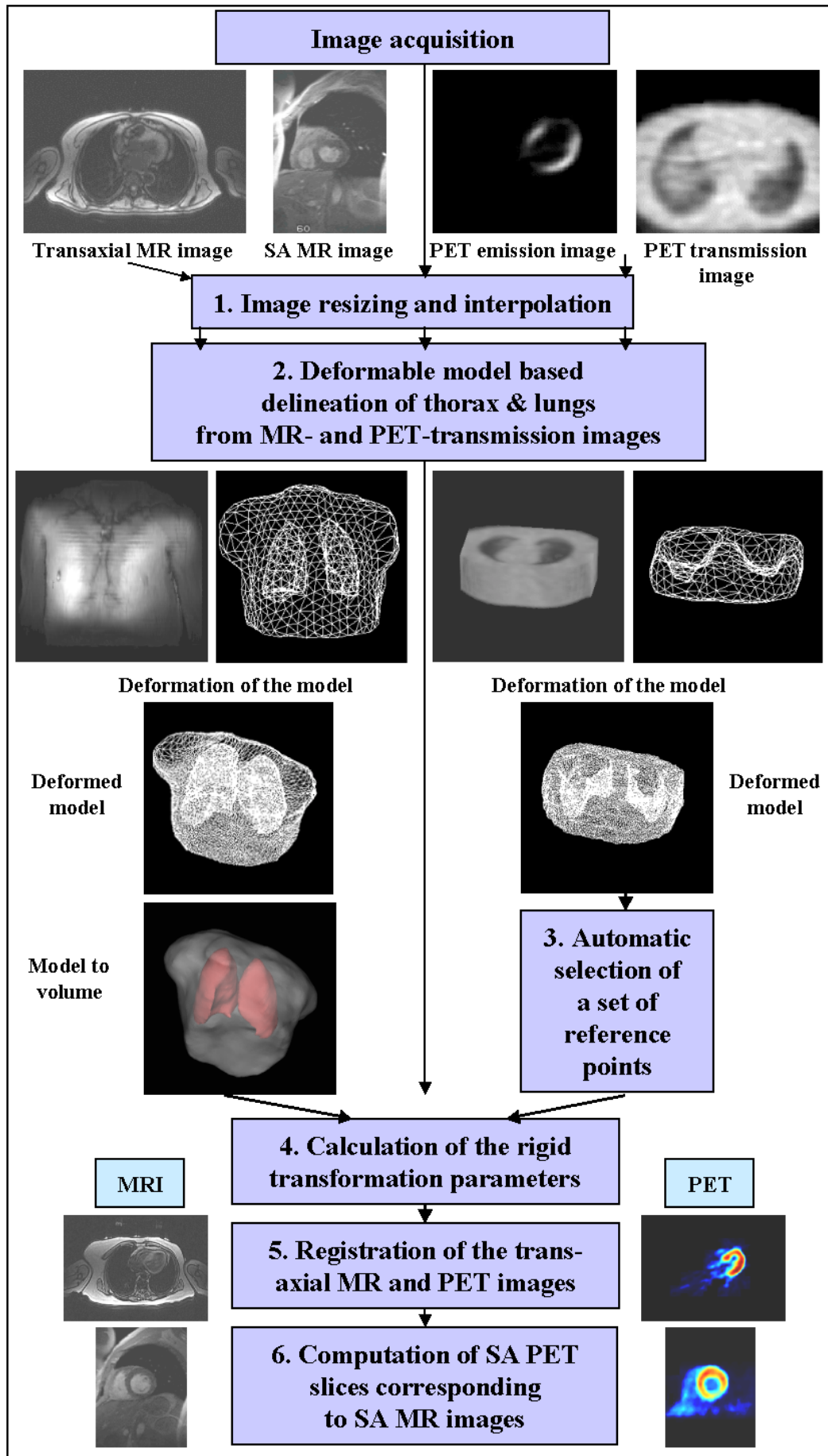
Figure 6: The main steps of the rigid MR and PET image registration method.

3) Automatic selection of a set of points from the segmented surfaces of the thorax and lungs in the PET model. The uniformly distributed nodes of the deformed model were used (Lötjönen et al., 1998).

4) Calculation of the rigid registration parameters (3 translations, 3 rotations) to find the best registration between the point set and the surfaces of the segmented MR image, by using the chamfer matching method (Borgefors, 1988).

5) Registration of the FDG PET emission image to the transaxial MR image coordinates was obtained using the computed registration parameters.

6) Registration of the SA MR images with FDG PET emission data. Information about slice positions in the MR image header provided the transformation between transaxial MR and SA MR slices. The SA FDG PET emission slices corresponding to SA MR images were computed from the registered transaxial images using the header information.

Segmentation

Segmentation of the thorax structures in Publication II was based on the elastic deformation (free form deformations) of a topologic and geometric prior model using a multi-resolution approach as presented in (Lötjönen et al., 1999). A thorax model including triangulated thorax and lung surfaces was used with transaxial MR images (Fig. 7a). With the transmission PET images, due to the reduced field of view, a truncated model with only a part of the thorax was used (Fig. 7b).
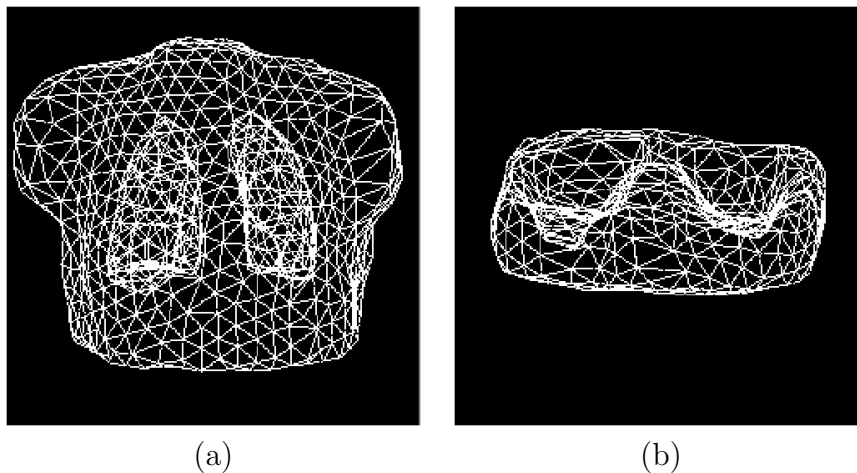

(a) (b)

Figure 7: Geometric and topologic prior model of the thorax for (a) transaxial MR and (b) transmission PET image segmentation (Publ. II, Publ. III) .

The deformation algorithm adapted the prior model to locally fit the salient edges in the image within a minimization process. The energy to be minimized was;

$$E_{total} = E_{image} + \gamma E_{model}, \tag{1}$$

where E_{image} represents the registration error between the prior model and the partial edges in the image. The energy term E_{model} tends to preserve the model's shape by restricting the deformation of the prior model. It describes the deviation of the model's surface normal from its original orientation. The parameter γ sets the contribution of the two energy components between zero and one. A multi-resolution approach was utilized for the minimization of the energy function. The image energy was calculated using oriented distance maps (Lötjönen et al., 1999) built upon extracted edges obtained from the Canny-Deriche edge detection (Canny,

1986; Deriche, 1987) or from image thresholding. In practice Canny-Deriche edge detection was utilized with MR images and with most of the PET transmission images. Thorax and lungs borders were in general well detected (visual inspection) from both MR and PET transmission images even though in PET transmission image edges are smoother than in MR images. With MR images the maximum error of 7-10 voxels (and average error of 1 voxel) has been obtained for deformable models based segmentation results while compared to MR volumes segmented by an expert (Lötjönen et al., 1999).

Computing the optimal registration transformation

The optimization of the rigid registration parameters was performed using a non-standard method, referred to here as the *grid optimization method* (Publ. II). The optimal registration parameters minimize the distance of a set of node points from the PET transmission image surface and the surface of the segmented MR image. The distances between the transformed node points and segmented MR surfaces were calculated using the chamfer distance map algorithm (Borgefors, 1988). In Fig. 8, an example of MR distance maps is presented.

Figure 8: MR distance maps. The registration algorithm minimizes the MR thorax surface distance with points of the PET transmission image surface by using the distance map (Publ. III).

In the grid optimization method a optima of 6 parameter vector was searched iteratively in the discrete search space. The search space was first divided using a user defined density grid (see Publication II for details). Registration error was calculated for each node point of the grid. A user-defined number of combinations, having the lowest registration error, were selected for the new initial parameter vectors for the denser grid. Iterations were repeated until the cost function did not decrease by more than a user-predefined value. The algorithm did not necessarily converge to the global minimum of the cost function. However, the method samples the search-space more than the basic gradient descent method and allows the minimum with a higher probability to be found. The method also allowed limited search space; it was possible to bound rotations and translations.

Evaluation of the rigid MR-PET registration method

The evaluation of the rigid MR-PET registration method in Publication II was mainly presented in Mäkelä et al. (2003) and is summarized here. In order to evaluate the registration method a reference PET-MRI data set was build up (Pauna et al., 2003). Transaxial MR images from the thorax of a healthy volunteer were acquired on a 1.5 T Siemens Magnetom Vision Imager (Siemens, Erlangen, Germany) at the Cardiological Hospital of Lyon. A series of 15 T1 weighted ECG-gated contiguous transaxial images covering the heart area were acquired during a breath hold sequence with a body array coil (Fig. 9a). The MR image was segmented and labeled (Fig. 9b). The result was inputted into a PET simulator. Simulated PET transmission (Fig. 9c) and FDG PET emission (Fig. 9d) images and original MR image provided the gold standard for registration.
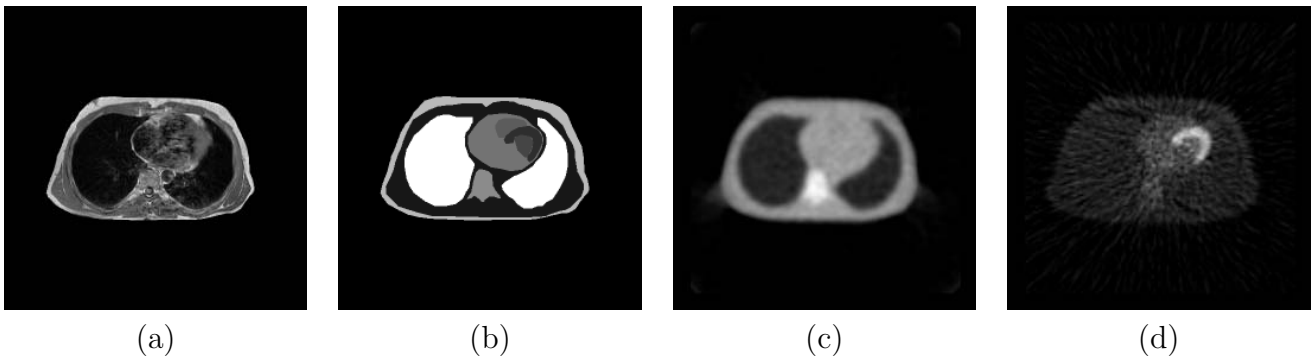

| (a) | (b) | (c) | (d) |

Figure 9: *(a) MR image, (b) segmented MR image, (c) simulated PET transmission and (d) FDG PET emission images (Mäkelä et al., 2003).*

The simulation of PET transmission and FDG PET emission images was performed using the SORTEO (Simulator of Realistic Tridimensional Emitting Objects) PET simulator (Reilhac et al., 2000, 2002). SORTEO is a Monte Carlo simulator, which uses a realistic 3-D software phantom based on MR images segmented into 9 classes (muscle, lungs, liver, fat, spine (bone), heart LV, the cavity of the LV, right ventricle (RV) and the cavity of the RV). It takes into account the specific activity and attenuation of each tissue. FDG PET emission image simulation was performed using an F-18 radioactive tracer. A PET transmission image simulation was obtained using Ge-68 as an external radioactive source. Reconstructed simulated PET transmission and FDG PET emission images (FBP with Hanning filter) had pixel sizes and slice thickness of 3.52 x 3.52 mm^2 and 2.43 mm, respectively. Both MR and simulated PET transmission and FDG PET emission images were interpolated (trilinear interpolation) to the same isotropic voxel size of 1.95 mm with 256 x 256 x 58 matrix size. Construction of the reference data set is fully described in Pauna et al. (2003).

Fifty transformations, obtained by randomly sampling the 6 parameter transformation vector, were applied to the PET transmission and FDG PET emission data. The translations were limited to $\pm$ 5 cm along each of the three axis and rotations around each axis ranged between $\pm$ 5 °. The selection of transformations followed Gaussian distribution and obeyed the previous constraints; N(0, 1.67)) cm for translations and N(0,1.67) degrees for rotations.

The fifty transformed simulated PET transmission images (and emission images) were registered with the reference MR image by using the surface based rigid registration method (Publ. II). The registration accuracy was evaluated by computing a Root Mean Square (RMS) error on all points belonging to the whole image area (number of points, n = 3801088), the thorax area (n = 907481), the heart area (n = 75944) and the LV area (n = 26517). The RMS error was obtained from the equation;

$$RMS = \sqrt{\frac{1}{n}\sum_{i=1}^{n} \parallel P_i - \hat{I}(T(P_i)) \parallel^2}, \tag{2}$$

where P_i is a voxel-point, $T(P_i)$ is the transformed voxel-point using the known transformations T, and $\hat{I}$ is the evaluated registration transformation calculated using the surface based registration method.

Results for the surface based registration of simulated images are presented in Table 2. Mean and standard deviation (SDV) values for RMS-errors were calculated for all four areas of interest. Two standard optimization methods, Powell and Simplex (Press et al., 1992), and one non-standard optimization method, referred to here as the *grid optimization method* (presented in the previous section), were tested. In the grid based optimizations the search space was limited to ± 25 voxel (about ± 5 cm) translations for all 3 directions (*x, y, z*) and ± 5 degrees of rotations around all three axis.

Table 2: *Registration accuracy (RMS-error in mm) for 50 tested transformations with the rigid surface based registration method. For each of the four areas of interest (whole image, thorax, heart and LV) mean RMS error and SDV using three optimization methods were calculated.*

Optimization	Whole image (n = 3801088) (mean ± SDV)	Thorax (n = 907481) (mean ± SDV)	Heart (n = 75944) (mean ± SDV)	LV (n = 26517) (mean ± SDV)
Grid	13.2 ± 3.4	10.7 ± 2.4	8.2 ± 2.3	7.7 ± 2.6
Powell	13.5 ± 4.2	10.9 ± 3.3	8.3 ± 2.9	7.8 ± 2.9
Simplex	14.9 ± 4.1	11.7 ± 3.1	10.5 ± 3.3	10.9 ± 3.6

Ten patient cardiac MR-PET image sets were also registered with the rigid surface based registration method. For estimating the results, visual analysis of the registered images were carried out for both the MR and PET transmission image registrations and then for MR and FDG PET emission image registrations. The results were visually satisfying in 9 of the 10 cases. In one PET image registration, unexpected artifacts in the FDG PET emission image was observed and the visual goodness of that registration result was difficult to confirm; the PET transmission image was also visually well registered in that case.

3.3 External markers based registration method for MR images and MCG data

The registration of MR images and MCG data relies on external markers. It was described in Publication III and in Publication V. The registration method is required for two purposes. Firstly in the inverse problem computations, the individual torso models, obtained from MR thorax images, are needed to be transformed into the coordinate system of the bioelectromagnetic measurement device. Secondly, the MCG solution of functional information of the cardiac electric excitation is needed to transform in the anatomy of the MR images.

The position of the MCG recording system with respect to the patient was determined by attaching three marker coils (magnetic dipoles) to the skin (Fig. 10). The magnetic fields produced by the coils were then used to compute the sensor locations relative to the marker coils (Montonen et al., 2000). The three marker coils were also used to define the MCG sensor

coordinates with respect to the nine MCG markers which were selected for registering the MCG sensor system to MR images.
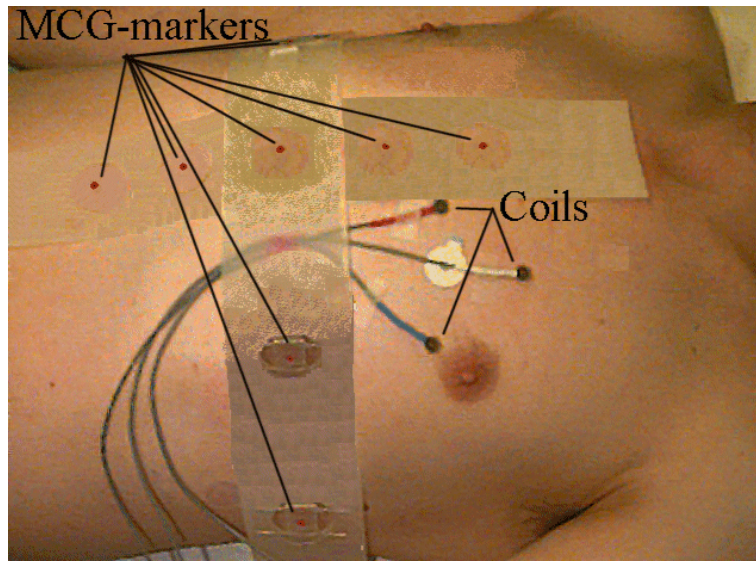

Figure 10: *Placements of the nine MCG markers and three marker coils on the chest in a typical patient study. The round pieces of plastic in two silicone strips of rubber denote the MCG marker locations. Their centrepoints are digitized, and thereafter the locations are stamped on the skin. The three marker coils are used to define the MCG sensor coordinates in respect to the MCG markers (Publ. III and V).*

The locations of the MCG markers and the small marker coils were defined with a 3-D digitization system (3SPACE ISOTRAK II, Polhemus Inc., Colchester, VT, USA) (Polhemus, 1993). The digitized MCG marker positions were stamped on the skin. Prior to MR imaging, the nine MRI markers were placed on the stamped positions on the skin. The MRI markers were constructed from two perpendicular tubes filled with 1 mmol/l $MnCl_2$ fluid, inserted inside a piece of plastic of $4.0 \times 4.0 \times 0.7$ cm. The cross-shaped figure of a marker was clearly visible in the MR images. The MRI markers were located manually from MR images, using dedicated software. The nine marker coordinate sets (x, y, z) in the MCG and MRI coordinate systems respectively, were registered using a non-iterative least-squares method (Arun et al., 1987). Only rigid transformations, including global rotations and translations, were considered.

In Publication V the relative impact of the different error sources in the MR-MCG registration method were evaluated. The objective of Publication V was to analyze the most severe error sources in the registration method, and to reduce their magnitude if possible. Measurements were made with a phantom and on a volunteer. The registration error includes various error sources and measurements were divided into five studies: A) the reproducibility of the 3-D localization using the digitization pen, B) the error in alignment of the patient, C) the error arising from repositioning of the MRI markers, D) the effect of different shapes in the measurement beds, and E) the localization error of the MRI markers from the images. The sum of all registration error components was about 6 mm and the contribution of different error sources to the total error was approximately equal.

3.4   Elastic registration method for cardiac MR and PET images

In Publication IV a novel method was developed for the elastic registration of two images. A combination of mutual information, gradient information and transformation smoothness was used to guide the deformation of the one image toward the other. The method was utilized for the registration of intra-patient cardiac MR and FDG PET emission images and inter-patient MR images of the head.

The elastic registration was achieved by maximizing the total energy, E_{total}, of the following energy function:

$$E_{total} = E_{MI} + \alpha E_{grad} + \beta E_{model}, \tag{3}$$

where E_{MI} and E_{grad} were respectively the mutual information and the joint gradient energy components (Pluim et al., 2000). The E_{model} was an energy component which constrained transformation so that they remained smooth (Rueckert et al., 1999). The terms α and β are user-defined weight parameters for the energy components.

The mutual information energy term E_{MI} measures the statistical dependence between two random variables or the amount of information that one variable contains about the other (Fitzpatrick et al., 2000; Hajnal et al., 2001; Maes et al., 1997; Wells et al., 1996; Woods, 2000a). The mutual information energy term can be qualitatively considered as a measure of how well one image explains the other. The mutual information is maximized at the optimal alignment and no assumptions are made regarding the nature of the relation between the image intensities in the registered images (Hill and Hawkes, 2000; Maes et al., 1997).

The energy component E_{grad} was derived from the gradients of the edges in the registered images. The joint gradient information comes from the assumption that the edges in the model should match either identical or opposite direction oriented edges in the data. The energy component E_{model} regularizes the transformation constraining transformation so that they remain smooth. Alternatively, if the surface model is available, the smoothness of the transformation can be controlled by constraining the change in the shape of the model surfaces.

The deformation of the images to be registered was accomplished within a multi-resolution process. The deformation of the images was done inside spheres with a varying position and radius. By default, the locations of the spheres are randomly chosen inside a model volume. The model volume with gray-scale information is elastically matched to a data volume. If a surface is not included in the model, only the smoothness of the transformation can be controlled. However, if the surface information is included in the model, the locations can be randomly chosen at the positions of the surface points. Also, if the surface is available, the method regulating the normal directions is recommended, because it makes the run time remarkably shorter. The model should contain surfaces for the regions which are required to be well matched in the final result. For example, if the thorax borders are to be registered from the image, the transformation inside and outside the borders are usually not of great interest. The use of the surfaces locates the deformation to the most interesting regions, and it speeds up the process because a great part of the volume is excluded, such as background. However, the spheres used at the lowest resolutions levels contain usually the whole or the most of the model volume, and allow therefore global transformation also for the regions far from the edges.

If model volume to be registered is an atlas, i.e. a volume where the tissue classes of the voxels are known, the result of elastic matching provides also a segmentation. The use of elastic models or deformable models, such as snakes, in the segmentation of cardiac images is a widely studied field in medical image processing (Frangi et al., 2001).

3.5   3-D functional maps

An approach for generating 3-D functional maps of the heart was presented in Publication III. The 3-D maps included information from registered MRI, FDG PET and MCG. To create maps, the SA MR image was segmented by using a bi-ventricular deformable heart model (Pham et al., 2001; Pham, 2002). The endocardial and epicardial boundaries were simultaneously extracted from SA MR images by a 3-D elastic deformation template. The medial surface was automatically calculated between the LV endo- and epicardial surfaces of the model. Calculation of the medial surface was done by firstly computing a normal to each node of the endocardial surface and secondly by calculating the middle point between the endocardial surface and the normal intersection with the epicardial surface (Fig. 11).
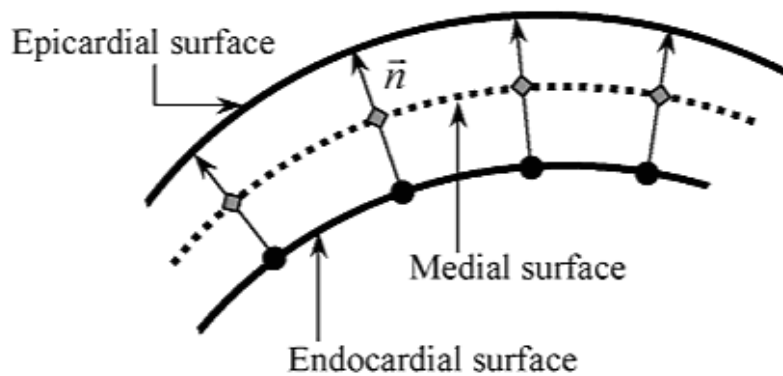

Figure 11: *The medial surface calculation (Publ. III).*

The model with the medial surface was then transformed from the SA MR image into the registered PET-FDG emission image and a FDG uptake mean value was computed at each surface node of the medial surface in a 5 x 5 x 5 neighborhood (Fig. 12). As a result the FDG metabolic activity over the LV medial surface together with the right ventricular and pericardial surfaces was combined to form a 3-D representation of the heart anatomy together with FDG uptake values. To obtain corresponding 3-D MCG functional maps, MCG inverse current-density estimates were calculated for the nodes of the medial surface.
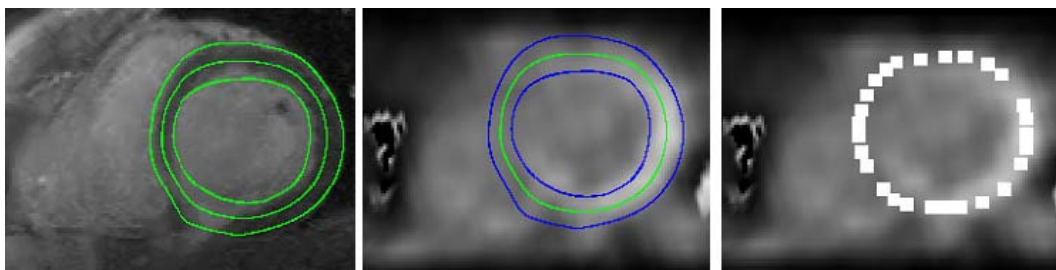

Figure 12: *(a) Intersection of endocardial (innermost contour), epicardial (outermost contour) and calculated medial (middle contour) surfaces using MR SA image, (b) the same contours are shown in the corresponding registered FDG PET SA image (medial contour in middle) and (c) the mean value of the FDG-uptake was computed at the medial surface nodes in a small neighborhood (Publ. III).*

3.6   Applications to cardiac studies

Data sets of ten MR and PET transmission and FDG PET emission images were rigidly registered in Publication II. In Figs. 13 and 14, rigidly registered end-diastolic MR and FDG PET emission images are presented for the case E1 in the transaxial and in the SA planes respectively (see Publication II for details).
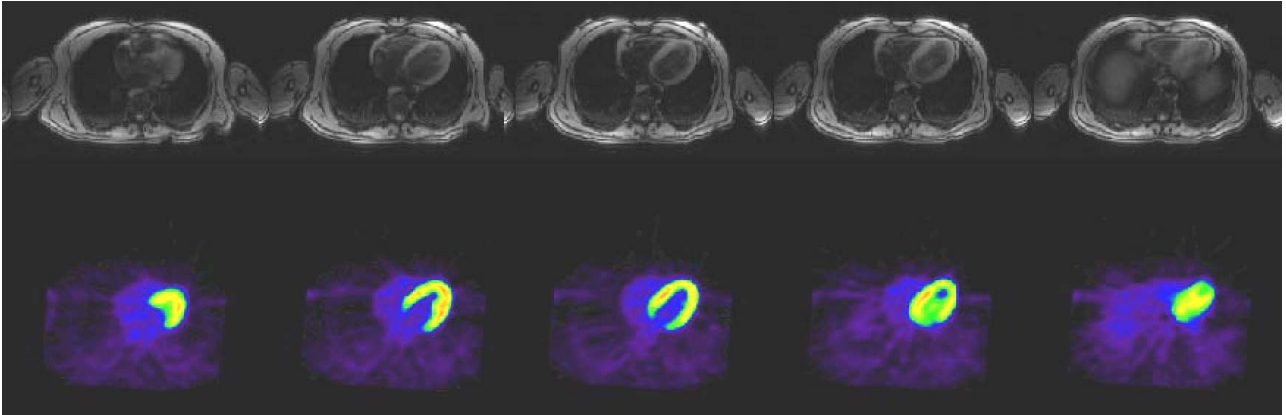
Figure 13: *Registered transaxial end-diastolic MR (top) and FDG PET emission (bottom) image slices for the E1 case (Publ. II).*
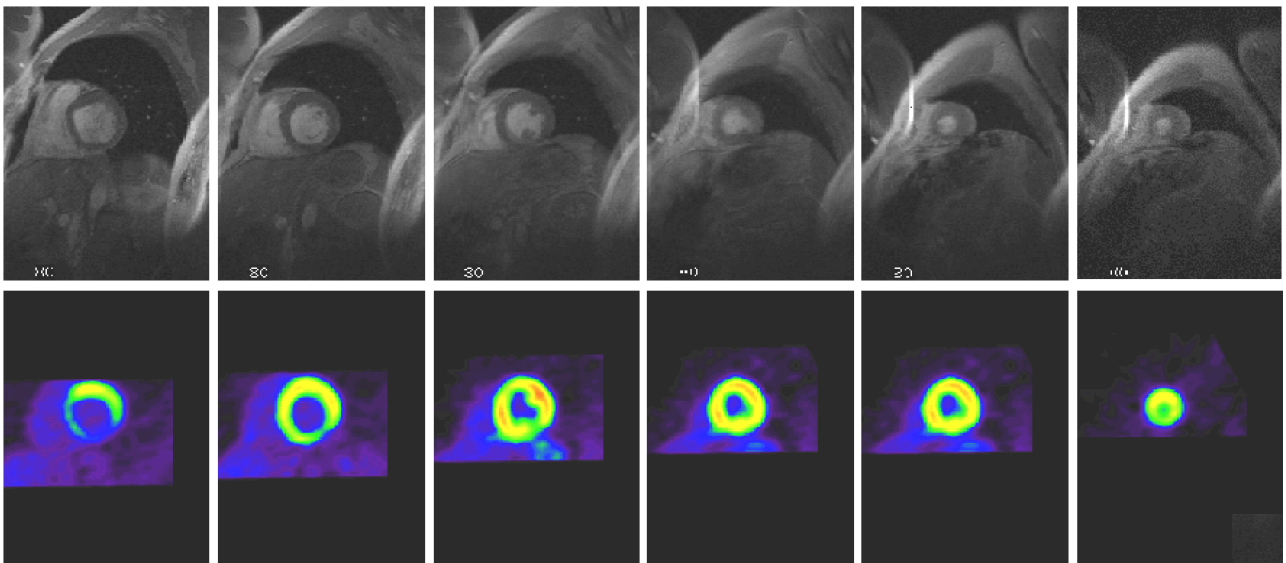
Figure 14: *Registered end-diastolic SA MR (top) and FDG PET emission (bottom) image slices for the E1 case (Publ. II).*

Fig. 15 (left) illustrates the FDG PET metabolic activity and MCG results (middle) over the LV medial surface for case E1. Right ventricular and pericardial surfaces are shown in transparency. The low LV FDG uptake areas can be seen in dark blue and low MCG values in dark green colors in the 3-D displays. For the initial evaluation of the method, the results were compared to manually made polarmap (bull's eye) presentations (Fig. 15) (right) (Publ. III).

Fig. 16 presents the result of the elastic registration of SA MR and SA FDG PET emission images. As an initialization, the SA FDG PET emission images were interpolated to SA MR voxel dimensions.
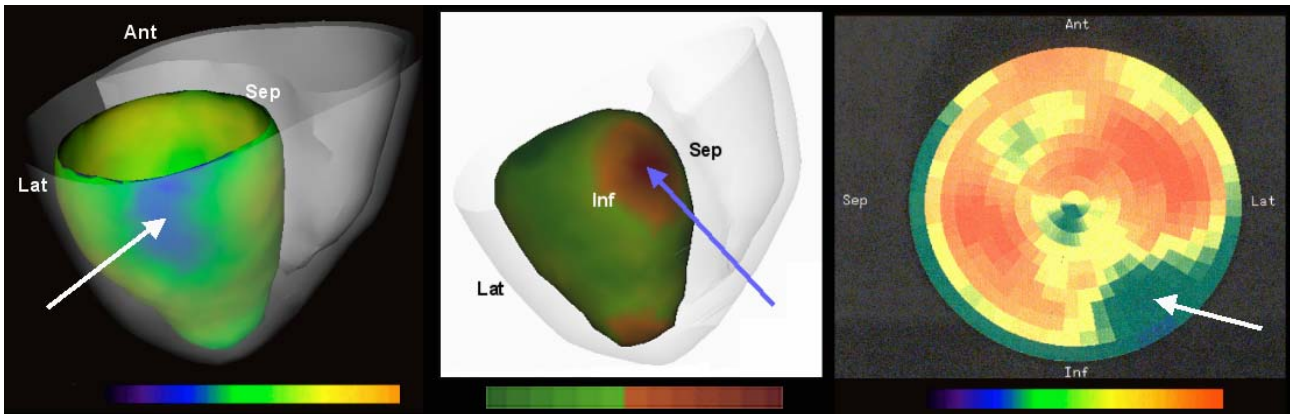
Figure 15: *3-D representations of the FDG PET uptake (left) and MCG values (middle) on the biventricular heart model of the patient E1. For comparison and evaluation of the method the manually made polarmap presentation (Siemens -software, Turku PET Centre) of the corresponding FDG PET image is presented on the right. A postero-laterobasal scar area can be seen coloured in blue (dark) in the basal level of the 3-D representation (left arrow) and in green (gray) in the polarmap image (right arrow). In the MCG data (middle) highest current magnitudes can be seen in red at the basal level of the presentations (arrow) and lowest current magnitudes in dark green (Publ. III).*

Figure 16: *Elastic registration of SA FDG PET emission and SA MR images for patient E3. After coarse registration result (up) and elastic registration result (down). Arrows in the images show one area where elastic registration clearly improved registration (Publ. V).*

4   Discussion

The registration of cardiac images is a complex problem, partly due to image acquisition conditions. Some acquisition constrictions and possible solutions are reviewed:

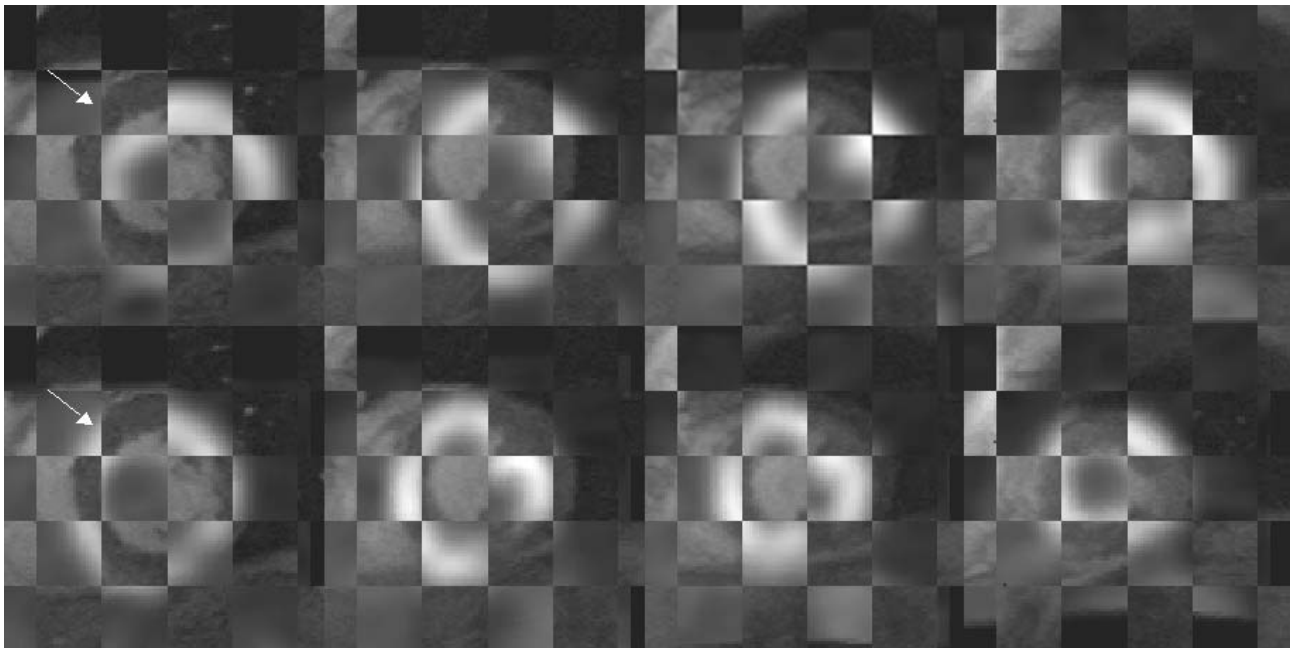1) In the rigid registration method in this thesis an assumption was made that the patient did not move in the MR imaging scanner during or between transaxial and SA MR image acquisitions. It was also assumed that the patient did not move during or between PET transmission and FDG PET emission imaging. In the cardiac MR imaging, the fixing of body relative to the surface coil might prevent the motion of the patient. Patient fixing systems such as vacuum cushions could also be used to reduce movement artifact during PET transmission and FDG PET emission imaging. Acquisition of the PET transmission images before and after the FDG PET emission image would also give an estimation of patient movement during and between the image acquisitions (Bettinardi et al., 1993). This would enable motion correction, but it would unfortunately also increase the radiation dose to the patient. Methods have also been presented for the registration of FDG PET emission and transmission images (Bettinardi et al., 1993; Costa et al., 1994). Also improved algorithms have been presented for shortening PET transmission imaging time and thus reduce the likelihood of movements artifacts during transmission imaging (Alenius et al., 1999). In general perfect match between transmission and emission studies is critical in whole-body studies where attenuation correction is crucial due to the presence of heterogenous tissues (mucle, bone, lung, etc.) (Bettinardi et al., 1993).

2) ECG-gated transaxial MR images of the ten patients were obtained using a snapshot technique during free respiration, and imaging of the whole thorax took about 1 minute. In comparison, PET transmission images can be seen as an integral image over the acquisition time (about 20 minutes). This might lead to differences in the thorax shape and diaphragm position between these two imaging methods. Registration in the rigid method was based on the delineation of the thorax and lung surfaces and therefore, the diaphragm should have similar positions in both imaging modalities. A possible solution could be similar breath gating (or breath holding in short sections) procedures in both imaging modalities or the use of the elastic registration methods. In general the bottom of the lungs were well visible in all of the 10 patient PET transmission images. In five images there were very small portition of the bottom of other or both lungs which were not visible in the PET transmission images. In these cases the deformable model approximates bottom of the small part of the lung bottom and this can cause error in registrations.

3) The registration of SA MR and FDG PET emission images was performed between end-diastolic cine MR images and ungated FDG PET images. The end-diastolic time point of cine MR images was selected because the ungated FDG PET images resulted from the uptake integration over several heart cycles, and mostly represented the diastolic phase. Gated PET emission images would help the registration by reducing the effect of the cardiac motion on the registration method. Gated PET emission images would also provide functional information during the heart cycle.

4) As the patients arms would attenuate the signal in PET transmission and emission imaging, they were held above the head during the imaging. This might change the position of the heart and lungs compared to MR imaging, where the patients keep their hands down beside the body (Dahlbom and Huang, 2000). It was not possible to use the same patient position in the MR imager as was used in the PET scanner because the duration of MR imaging for viability studies can last up to 60 minutes. Also, the diameter of the MR imagers tube is too small for some patients to lie in this position. Elastic registration techniques could help to solve small anatomical differences in these situations (Tai et al., 1997).

5) The utilized MR and PET images pose several requirements for the registration. The

registration algorithm did not necessarily converge to the correct result if the initial parameter vector was too far from the optimal result. With the PET transmission and MR transaxial images used for the calculation of the rigid transformation the initial parameter vectors were close enough for the algorithm to converge, and, for example, manual repositioning of the images before registration was not needed. The surfaces extracted should not present rotational symmetries (e.g. for cylindrical objects the solution is not unique) which was usually not the case with the thorax including lungs. Every surface point used in registration should have a unique corresponding point in the other image. In patient PET transmission and FDG PET emission images there was smaller field of view than in MR images. Therefore in some cases part of the PET transmission image surface points were excluded semi-automatically from the calculation of the registration parameters if they had no corresponding edges in MR images.

6) Patient MR images covered the whole thorax area while MR, PET transmission and FDG PET emission images used for registration method evaluation only covered the heart area. In patient PET transmission images the bottom of the lungs were in general more clearly visible than in simulated transmission images and thus helped the surface based registration of the patient images. Also, the larger imaging area of patient MR images (the whole thorax) could also help with registration when compared to simulated images where only the heart area was imaged. However, simulated images did not included movement artifacts caused by breathing, cardiac movement and patient movement which are all present in patient images. In patient MR images the imaging time was too long (about 1 minute) for patient breath holding because the whole thorax area was imaged. For MR images used in the PET simulator only the heart area was covered and breath holding was used. The hands were segmented from MR images used in the PET simulator as during patient PET transmission and FDG PET emission imaging hands are normally hold above the head to avoid extra attenuation in the cardiac area. Simulations of PET images (emission, transmission) were done from segmented MR images as an input. The segmentation of the MR images (into 9 classes) is prone to errors and can therefore cause some differences in simulated images when compared to the original MR image.

The rigid surface based registration method in MR and FDG PET images was evaluated with simulated images and with data obtained from ten patients. Surface based methods are efficient registration methods when registered structures are clearly visible and thus easy to segment. They in principally do not require *a priori* knowledge of the nature of registered images or information from intensity distribution of images. The accuracy of the surface based methods is mainly depended how accurately surfaces used for registration can be extracted from images. The results of the surface based registration with simulated images (Table 2) showed that the RMS error was greater than the voxel size of the registered images (isotropic 1.95 mm) with all optimization methods in all four studied areas (whole image, thorax, heart and LV). The best results for the surface based registration of 50 cases looking at the heart area were obtained with the grid optimization method with a RMS error of 8.2 ± 2.3 mm. In the surface based registration method with grid optimization the search space was limited to $\pm$ 25 voxel (about $\pm$ 5 cm) translations from the original position for all directions and $\pm$ 5 degrees for rotations around all three axis. With the registration of patient images grid based optimization with limited search space gave also visually satisfying results in 9 of the 10 cases. In one patient case the registration of transmission image was successful but there were unexpected artifacts in the FDG PET emission data. Probable reason for the problems in FDG PET emission data was movement artifacts between (or during) PET transmission and FDG PET emission imaging. With patient images grid optimization method was the most robust while considering visual inspections; two cases of ten registration with both Powell and Simplex minimizations were visually unsatisfactorily registered. One probable reason for robustness of grid method was that the limited search space allowed only reasonable results.

The developed rigid registration method in FDG PET and MR images differs from the previously introduced methods (e.g. Pallotta et al. (1995); Gilardi et al. (1998)), especially as it has an automatic deformable model based segmentation of thorax and lung surfaces derived from both the PET transmission and thorax MR images. Another advantage of the registration method was that it not only provided registered transaxial images but also SA images, which have clinical importance in cardiology. The registration method could be applied to MR-SPECT or PET-SPECT image registration as well if also the SPECT transmission image is available. Gated cardiac PET emission images would also improve registration results, allowing the similar cardiac phases to be registered between MR and PET emission images.

The speed of registration algorithm depends on factors like the need of the preprocessing, the complexity of the cost function and the number of the cost function evaluations performed by the optimization algorithm (Bankman, 2000). Compared to the ICP algorithm (Besl and McKay, 1992) the presented surface based MR-PET registration approach also requires the segmentation of the data. In surface based registration method, the distance map is computed once as a preprocessing step and after that the estimation of the distances between the model and the data points is immediate. In the ICP algorithm the distances between surfaces are explicitly computed at every iteration. Thus when chamfer distance map algorithm is compared to ICP algorithm it has lower cost function complexity but it requires more preprocessing (Bankman, 2000). With patient images automatic segmentation of the MR and PET transmission images with the size of 256 x 256 x 217 voxels took less than 3 minutes on a PC workstation (PIII, 800 MHz). With the same image size, the execution time for registration (grid optimization) was about 50 seconds when using about 1000 points to compute the rigid transformation parameters. In our experiments the proposed registration parameter search strategy of grid optimization method provided a fast and reliable results.

The rigid surface based registration method (Publ. II) was also compared with rigid voxel similarity based registrations with mutual information (Maes et al., 1997; Wells et al., 1996), normalized mutual information (NMI) (Studholme et al., 1997, 1999) and a correlation ratio (CR) (Roche et al., 1998, 2001) in Mäkelä et al. (2003). Image intensity based methods do not need *a priori* extraction of registered structures (e.g. segmentation of surfaces) and are thus promising methods for the automatic registration of images. Mutual information is an information theory measure of the statistical dependence between two random variables or the amount of information that one variable contains about the other (Fitzpatrick et al., 2000; Hajnal et al., 2001; Maes et al., 1997; Wells et al., 1996; Woods, 2000a). Mutual information can be qualitatively considered as a measure of how well one image explains the other. The mutual information is maximized at the optimal alignment (Hill and Hawkes, 2000). No assumptions are made regarding the nature of the relation between the image intensities in the registered images (Maes et al., 1997). Therefore, the mutual information method is promising in particular for intermodality registration. In CR measure (Roche et al., 1998, 2001) one image is considered as an model of other image and functional dependency is assumed between image intensities. The registration results of image intensity based methods using simulated MR-PET images were evaluated in similar manner than with the surface based registration method (Section 3.2). Most accurate results (when also compared with surface based registrations) were obtained with NMI and CR voxel similarity based registration methods. For NMI and CR with simplex optimization, the RMS error for the heart area with 50 isotropic simulated images was 2.9 ± 0.5 mm and 2.9 ± 0.4 mm, respectively. Registration with mutual information based registration failed (visually checked) in several cases and the RMS error was more than ten times bigger than with NMI and CR. While the RMS error of rigid surface based registration method with limited search space was 8.2 ± 2.3 mm, the comparison of registration accuracy with voxel similarity based registration methods showed that the surface based registration method

performed better than mutual information based method, and that the registration accuracy of the surface based registration method was lower than the accuracies of NMI and CR methods. When registering emission images directly with MR images using mutual information, NMI and CR image intensity based methods, only about fifth of the cases succeeded (visual inspection) while considering registrations with both simulated images and patient images. Thus, results indicated that the use of transmission image as a linking mediator is more accurate and reliable way to register FDG PET emission images and MR images.

In Publication III an approach for the 3-D visualization of anatomical and functional information from registered MR and FDG PET images and MCG data was developed. The data fusion method combined structural information from MR images and functional information from FDG PET and MCG. With presented approach, the localization of metabolic and conduction defects is straightforward since the biventricular model with LV medial surface allows for the unambiguous identification of myocardial territories. In the literature, electrical activity and metabolism have usually been studied separately, principally because the acquisition system are quite different and involve different specialists. From the physiopathological point of view, it is clear that all the activities are related one to each other. Therefore, our objective here was to allow for the study of the correlation between the electrical (MCG data) and metabolic (FDG PET imaging) activities which may reveal new aspects of hearts complex pathological processes. The data fusion method gave good spatial understanding of myocardial FDG uptake information and MCG values of the heart and might help to make better clinical diagnosis e.g. in viability studies (Nenonen et al., 2001). The presented 3-D method gives good possibilities especially for visual comparison of data from different imaging modalities. Within the same framework, it is natural to envisage the inclusion of other complementary functional data such as information related to the myocardial deformation or perfusion and also to temporal information by using e.g. gated FDG PET image acquisitions (Behloul et al., 2001). The reliability of the method depends on the accuracy of the rigid PET-MRI registration and the accuracy of the segmentation of the heart structures and extraction of LV medial surface. Methods accuracy also depends on the data modalities utilized. PET imaging devices have typically 4 - 10 mm spatial resolution (Hartiala and Knuuti, 1995). In MCG, accuracies of 5 to 25 mm have been reported by comparing the MCG localization results to: i) cardiac surgery, ii) catheter ablation, iii) the results of invasive electrophysiological studies, iv) ECG localization results, and v) physiological knowledge (X-ray or MRI) (Fenici et al., 1998; Pesola et al., 1999). The presented the 3-D visualization method with LV medial surface seems the most straightforward way to obtain LV functional cartographies preventing from border effects that could occur from slight mis-registration.

The elastic registration method was developed in Publication IV. In the elastic registration method qualitative visual analysis of the elastically registered cardiac SA MR-PET images were satisfactory for the tested cases. Elastic registration methods can, for example, reduce the effect of the small differences in thorax and heart shapes between registered images. However, the evaluation of the method was only carried out visually, and more extensive validation with, for example, simulated images has to undergone.

The error analysis for the external marker based registration method for anatomical MR data with functional MCG data was presented in Publication V. The relative strengths of the different error sources were evaluated. The sum of all the registration error components was 6 mm. The error value explained well the RMS error of the nine registered markers in our 50 patient studies where the error was obtained also to be about 6 mm (Pesola et al., 2000). A drastic reduction of the total RMS error would not be easy to accomplish because any error sources appeared to dominate. However, the effect of the differences in measurement bed shapes could be reduced by making a firm support which copied the shape of the MRI bed and could

be used during MCG digitizations. Also, the use of oblique slices appeared to be superior to orthogonal slices when defining MR markers from images. The use of breath holding during the MR imaging (e.g. in short sections) and the 3-D localization of the MCG markers could also help to reduce registration error.

In Publication VI the combined results of three MR imaging modalities (dobutamine stress cine, first pass and late contrast material-enhanced T1-weighted imaging) were compared with FDG PET results in the assessment of unviable myocardium in coronary artery diseases. The FDG PET data were used as reference material in order to analyze the ability of the MR methods to detect unviable myocardium areas. The visualization of the registered MR-PET images clearly showed decreased activity in the possible infarction areas. The combination of first-pass enhancement analysis and wall motion assessment with stress significantly increased the specificity of MR imaging in the detection of unviable sectors.

5 Conclusions

Several aspects related to the cardiac image registration and data fusion methods were presented and discussed in this thesis from methods developments and implementation to clinical cardiac studies. This thesis consisted of an overview of the above including also new material, and of six publications. New methods were developed, particularly for the registration and data fusion of MR and FDG PET images and MCG data. Registration and data fusion methods performed well in general, but generating 3-D functional maps presenting anatomical and functional information was very time-consuming; it needed registration, segmentation, calculation of MCG values and then data fusion with 3-D visualizations. Alternative methods do exist, especially in the area of registration of multimodality data.

The choice of a cardiac image registration method is a difficult one since a generally applicable method for registering images does not exists. External skin marker based registration of cardiac images does not guarantee registration of the heart within the body because of heart movement and movement of thorax structures. Landmark based registration of the heart is difficult because there are not many spatially accurate anatomical landmarks in cardiac images and they can also be less visible with certain modalities and in some pathological conditions, such as ischemia. Surface based registration methods utilizing the thorax outline can sometimes be used if it is not possible to obtain structural information from the heart surfaces directly. With thorax surface based cardiac image registration methods using both thorax and lungs surfaces, which are clearly visible in thorax MR and CT images and in PET and SPECT transmission images, is recommend (Pallotta et al., 1995). Nevertheless, these methods are prone to errors induced by respiration and different movement artifacts (Goerres et al., 2002). Direct registration of the heart surfaces can result in better registration of the area of interest, but the choice of the surfaces to be registered is important and depends on the application and modalities used. The voxel similarity measures, compared to geometric image feature based registration methods, have an important advantage in that they do not require *a priori* extraction of the features (e.g. segmentation). In modern information theoretic voxel similarity methods, such as mutual information, little assumptions are made regarding the nature of the relation between the image intensities in the registered images (Maes et al., 1997). These methods are particularly promising for multimodality cardiac image registration. Taking into account our preliminary experiments (Mäkelä et al., 2003) it would seem that multimodal cardiac MR-PET image registration, with NMI and with CR, gave more accurate results than the rigid thorax surface based registration of the images. Because of the very recent development of the mutual information based registration methods, applications to cardiac image registration are still rare.

Rigid cardiac image registration generally does not describe the spatial relationship between images adequately. Elastic cardiac image registration is needed largely as a consequence of cardiac motion; between end-diastole and end-systole (during cardiac cycle) the heart valvular plane moves 9-14 mm towards the apex, and the myocardial walls thicken from approximately 10 mm to over 15 mm (Rogers et al., 1991; O'Dell et al., 1995; Klein and Huesman, 2002). Further, the problems due to imaging conditions, different movement artifacts and elasticity of the body, lungs and the heart cause different tissue deformations which are not possible to compensate for with rigid registration methods. Elastic methods would also be useful in atlas based methods, where large datasets would be registered to the same atlas, allowing statistical information relating to the functional and structural parameters to be collected (Thirion, 2001).

In this thesis methods for data registration and fusion in cardiac applications were developed. A rigid registration method was developed to combine anatomical information from MR, and metabolic information from FDG PET. The registration method was evaluated with simulated images and applied to 10 patient cases. The method has been applied to research purposes

in (Publ. III, Nenonen et al. (2001)) as well as clinical studies (Publ. VI). A developed elastic registration method was applied for the registration of intra-patient cardiac MR and FDG PET images and inter-subject MR images of the head. Method gave visually satisfactory results for both cases. The elastic registration method can compensate small differences caused by heart motion and shape variability's in inter-subject studies. The 3-D model based approach was developed to combine anatomical information from MR and functional information from FDG PET and MCG. The data fusion method gave good spatial understanding of myocardial FDG uptake information and MCG values of the heart, and can help to make better clinical evaluations, e.g. in viability studies. For registering MR images and MCG data external markers based rigid registration method was utilized. In this work also different error sources for MR image and MCG data registration methods were evaluated with volunteer studies and phantom experiments. Obtained results can help to reduce registration error in the MR-MCG registration method. Finally, improved analysis of MR and FDG PET images and MCG data was obtained employing the presented methodology.

6 Summary of publications

I T.J. Mäkelä, P. Clarysse, O. Sipilä, N. Pauna, Q.C. Pham, T. Katila and I.E. Magnin (2002). A review of cardiac image registration methods. *IEEE Trans. Med. Imaging* 21:1011-1021.

In this review the current status of cardiac image (MRI, CT, PET, SPECT and US) registration methods was presented, and implementation and validation issues were discussed. Registration of these modalities has become of increasing interest in the medical community for physiologic understanding and diagnostic purposes. There are numerous specific problems in cardiac image registrations, mainly related to the different motion sources (patient, respiration and heart) and to the specificity of each imaging modality. To date, no general method exists to automatically register any modality with any other modality. Modern information theoretic voxel similarity based registration methods, such as mutual information, are particularly promising for the intramodality cardiac image registration. Elastic cardiac image registration methods are also needed because rigid cardiac image registration generally does not describe the spatial relationship between cardiac images adequately.

II T.J. Mäkelä, P. Clarysse, J. Lötjönen, O. Sipilä, K. Lauerma, H. Hänninen, E.-P. Pyökkimies, J. Nenonen, J. Knuuti, T. Katila and I.E. Magnin (2001). A new method for the registration of cardiac FDG PET and MR images using deformable model based segmentation of the main thorax structures. In *Proc. of the 4nd International conference on Medical Image Computing and Computer Assisted Intervention (MICCAI'01)*. W. Niessen, M.A. Viergever (Eds.). Springer. *Lect. Notes Comput. Sci.* 2208:557-564.

A method for the rigid registration of cardiac MR and FDG PET images was developed. The method was based on the registration of the surfaces of thorax structures extracted by a deformable model from PET transmission and MR transaxial images. A MR short axis registration with a FDG PET emission image was also derived and used to study viability in proper anatomical conditions. The method was tested in 10 patient cases and the registration results were visually satisfying in 9 of the 10 cases. In one case, registration was successful with transmission images but there were unexpected artifacts in the FDG PET emission data.

III T.J. Mäkelä, Q.C. Pham, P. Clarysse, J. Nenonen, J. Lötjönen, O. Sipilä, H. Hänninen, K. Lauerma, J. Knuuti, T. Katila and I.E. Magnin (2002). A 3-D model-based registration approach for the PET, MR and MCG cardiac data fusion. *Medical Image Analysis*, accepted for publication.

An approach for creating 3-D functional maps of the heart was developed. The data fusion method combines structural information from MR images, and functional information from FDG PET images and MCG data. The method utilized surface based registration from MR and PET images and the external marker based registration of MR images and MCG data. The extraction of an individualized anatomical heart model from MR images was done using deformable models. The 3-D data visualizations gave good spatial understanding of myocardial FDG uptake information and MCG values of the heart, and can better help make clinical evaluations, e.g. in viability studies.

IV J. Lötjönen and T.J. Mäkelä (2001). Elastic matching using a deformation sphere. In *Proc. of the 4nd International conference on Medical Image Computing and Computer Assisted Intervention (MICCAI'01)*. W. Niessen, M.A. Viergever (Eds.). Springer. *Lect. Notes Comput. Sci.* 2208:541-548.

A novel method was developed for the elastic registration of two images. A combination of mutual information, gradient information and smoothness of the transformation was used to guide the deformation of one image towards another image. The deformation was accomplished within a multi-resolution process by spheres containing a vector field. The feasibility of the elastic registration method was demonstrated in two cases: registration of intra-patient cardiac MR and FDG PET images and inter-patient MR images of the head. Qualitative visual analysis of the elastically registered images were satisfactory for the tested cases.

V T.J. Mäkelä, J. Lötjönen, O. Sipilä, K. Lauerma, J. Nenonen, T. Katila and I.E. Magnin (2002). Error analysis of registering of anatomical and functional cardiac data using external markers. In *Proc. 13th Int. Conf. on Biomagnetism (BIOMAG'02)*. H. Nowak, J. Haueisen, F. Giesler, R. Huonker (Eds.). Verlag. Pages 842-845.

In this work the relative strengths of the different error sources in a skin marker based registration method for functional MCG data and anatomical MR images of the heart were evaluated. The objective was to analyze the most severe error sources in the registration method and to reduce their magnitude if possible. The error sources were divided into five studies: A) the reproducibility of the 3-D localization using the digitization pen, B) the error in alignment of the patient, C) the error arising from repositioning of the MRI markers, D) the effect of different shapes in the measurement beds, and E) the localization error of the MRI markers from the images. Measurements were made with a phantom and on a volunteer. The sum of all registration error components was 6 mm. No specific error sources dominated and their contribution to the total error was approximately equal.

VI K. Lauerma, P. Niemi, H. Hänninen, T. Janatuinen, L-M. Voipio-Pulkki, J. Knuuti, L. Toivonen, T.J. Mäkelä, M. Mäkijärvi and H.J. Aronen (2000). Multimodality MR imaging assessment of myocardial viability: combination of first-pass and late contrast enhancement to wall motion dynamics and comparison with FDG PET – initial experience. *Radiology* 217:729-736.

Three MR imaging modalities (dobutamine stress cine, first pass, and late contrast material-enhanced T1-weighted imaging) and FDG PET results were compared in the assessment of unviable myocardium in coronary artery disease. The registered FDG PET data was seen as a reference which could be used to analyze the ability of MR methods to detect myocardial viability. The combination of first-pass enhancement analysis and wall motion assessment with stress significantly increased the specificity of MR imaging in the detection of unviable sectors.

Author's contribution

All publications included in this thesis are result of a group effort. The majority of the work in Publication I was carried out by the author. For Publication II, the majority of the work concerning the design of the developed rigid registration method for FDG PET and MR images was done by the author. The author applied the deformable model based segmentation method and rigid registration algorithm for the 10 patient MR-PET studies. The deformable model based segmentation method was not developed in this work but the author implemented algorithms for the automatization of different steps in the rigid MR-PET registration method. In Chapter 3 the author evaluated the rigid cardiac MR-PET registration method by applying simulated cardiac MR-PET images. In Publications III the author designed the 3-D model based approach for obtaining structural information from MR and functional information from FDG PET and MCG, and registered MR and FDG PET images for this purpose. Additionally, in Publication III, the author participated in the design and implementation of most of the algorithms used to obtain the 3-D visualizations from the registered images, except for the segmentation method used to obtain the 3-D model and for the calculations of MCG values. For the visualizations in Publication III, the Visualization Toolkit Software (VTK) was used. In Publication IV the author applied the elastic registration method for cardiac MR and FDG PET images. In Publication V the author participated in the performance of the methods for estimating different sources of registration errors and for the calculations of results. The registration method for MR images and MCG data was not developed in this work. The rigid registration of MR and FDG PET images in Publication VI were carried out by the author. Publication I and II were written by the author and Publication III and V was mostly written by the author. The author also participated in the writing of Publication IV.

References

Alenius, S., Ruotsalainen, U., and Astola, J. (1999). Attenuation correction for PET using count-limited transmission images reconstructed with median root prior. *IEEE Trans. Nucl. Science*, 46(3):1011–1021.

Ambroggi, L., Musso, E., and Taccardi, B. (1989). *Comprehensive electrocardiology*, volume 2, chapter Body-Surface Mapping, pages 1015–1049. Pergamon Press.

Andersson, J. L. R., Bagnhammar, B., and Schneider, H. (1995). Accurate attenuation correction despite movement during PET imaging. *J. Nucl. Med.*, 36(4):670–678.

Arun, K. S., Huang, T. S., and Blostein, S. D. (1987). Least-squares fitting of two 3-D point sets. *IEEE Trans. Pattern Anal. Machine Intell.*, 9(5):698–700.

Audette, M., Ferrie, F., and Peters, T. (2000). An algorithmic overview of surface registration techniques for medical imaging. *Med. Image Anal.*, 4(4):201–217.

Bacharach, S., Douglas, M., Carson, R., Kalkowski, P., Freedman, N., Perrone, P., and Bonow, R. (1993). Three-dimensional registration of cardiac positron emission tomography attenution scans. *Computer Vision, Graphics and Image Processing*, 34(2):311–321.

Baer, F., Voth, E., and LaRosee, K. (1996). Comparison of dobutamine transesophageal echocardiography and dobutamine magnetic resonance imaging for detection of residual myocardial viability. *Am. J. Cardiol.*, 78:417–419.

Bankman, I. N. (2000). *Handbook of Medical Imaging: Processing and Analysis*. Academic Press.

Behloul, F., Lelieveldt, B. P. F., Boudraa, A., Janier, M., Revel, D., and Reiber, J. H. C. (2001). Neuro-fuzzy systems for computer-aided myocardial viability assessment. *IEEE Trans. Med. Imaging*, 20(12):1302–1313.

Besl, P. J. and McKay, N. D. (1992). A method for registration of 3-D shapes. *IEEE Trans. Pattern Anal. Machine Intell.*, 14(2):239–256.

Bettinardi, V., Gilardi, M., Lucignani, G., Landoni, C., and Rizzo, G. (1993). A procedure for patient repositioning and compensation for misalignment between transmission and emission data in PET heart studies. *J. Nucl. Med.*, 34(1):137–142.

Beyer, T., Townsend, D., Brun, T., Kinahan, P., Charron, M., Roddy, R., and Jerin, J. (1999). A combined PET/CT scanner for clinical oncology. *J. Nucl. Med.*, 41(8):1369–1379.

Bidaut, L. and Vallée, J.-P. (2001). Automated registration of dynamic MR images for the quantification of myocardial perfusion. *Journal of magnetic resonance imaging*, 13:648–655.

Borgefors, G. (1986). Distance transformation in digital images. *Computer Vision Graphics and Image Processing*, 48:344–371.

Borgefors, G. (1988). Hierarchical chamfer matching: A parametric edge matching algorithm. *IEEE Trans. Pattern Anal. Machine Intell.*, 10(6):849–865.

Brown, L. (1992). A survey of image registration techniques. *ACM Computing Surveys*, 24(4):325–376.

Brownell, G. and Sweet, W. (1953). Localization of brain tumors with positron emitters. *Nucleonics*, 11:40–45.

Budinger, T. and VanBrockling, H. (1995). *The biomedical engineering handbook*, chapter Positron Emission Tomography PET, pages 1134–1150. CRC Press.

Cai, J., Chu, J., Recine, D., Sharma, M., Nguyen, C., Rodebaugh, R., Saxena, A., and Ali, A. (1999). CT and PET lung image registration and fusion in radiotherapy treatment planning using the chamfer-matching method. *Int. J. Radiation Oncology Biol. Phys.*, 43(4):883–891.

Canny, J. (1986). A computational approach to edge detection. *IEEE Trans. Pattern Anal. Machine Intell.*, 8(6):679–698.

Carrillo, A., Duerk, J., Lewin, J., and Wilson, D. (2001). Semiautomatic 3-D image registration as applied to interventional MRI liver cancer treatment. *IEEE Trans. Med. Imaging*, 19(3):175–185.

Conolly, S., Macovski, A., and Pauly, J. (1995). *The biomedical engineering handbook*, chapter Magnetic resonance imaging, pages 1006–1014. CRC Press.

Costa, W., Haynor, D., and Lewellen, T. (1994). Registration of segmented attenuation and emission data in PET. In *Proc. of Nucl. Science Symposium and Medical Imaging Conference*, pages 1407 – 1411.

Dahlbom, M. and Huang, S.-C. (2000). *Handbook of Medical Imaging: Processing and Analysis*, chapter Physical and biological bases of spatial distortions in positron emission tomography images, pages 439–448. Academic Press.

Declerck, J., Feldmar, J., Goris, M., and Betting, F. (1996). Automatic registration and alignment on a template of cardiac stress and rest SPECT images. Research Report 2770, INRIA.

Declerck, J., Feldmar, J., Goris, M., and Betting, F. (1997). Automatic registration and alignment on a template of cardiac stress and rest reoriented SPECT images. *IEEE Trans. Med. Imaging*, 16(6):727–737.

Deriche, R. (1987). Using Canny's criteria to derive a recursively implemented optimal edge detector. *International Journal of Computer Vision*, 1:167–187.

Dey, D., Slomka, P., Hahn, L., and Kloiber, R. (1999). Automatic three-dimensional multimodality registration using radionuclide transmission CT attenuation maps: A phantom study. *J. Nucl. Med.*, 40(3):448–455.

Eberl, S., Kanno, I., Fulton, R., Ryan, A., Hutton, B., and Fulham, M. (1996). Automated interstudy image registration technique for SPECT and PET. *J. Nucl. Med.*, 37(1):137–145.

Faber, T., McColl, R., Opperman, R., Corbett, J., and Peshock, R. (1991). Spatial and temporal registration of cardiac SPECT and MR images: methods and evaluation. *Radiology*, 179(3):857–861.

Fenici, R., Nenonen, J., Pesola, K., Korhonen, P., Lötjönen, J., Mäkijärvi, M., Poutanen, V. P., Keto, P., and Katila, T. (1998). Non-fluoroscopic localization of an amagnetic stimulation catheter by multichannel magnetocardiography. *PACE*, 22:1210–1220.

Fitzpatrick, J., Hill, D., and Maurer, C. (2000). *Handbook of Medical Imaging*, volume 2, chapter Image registration, pages 447–513. SPIE Press.

Frangi, A. F., Niessen, W. J., and Viergever, M. A. (2001). Three-dimensional modeling for functional analysis of cardiac images, a review. *IEEE Trans. Med. Imaging*, 20(1):2–25.

Gallippi, C. M. and Trahey, G. E. (2001). Automatic image registration for MR and ultrasound cardiac images. In Insana, M. F. and Leahy, R. M., editors, *Lecture Notes in Computer Science 2082: Information Processing in Medical Imaging, IPMI01*, pages 141–147. Springer.

Gilardi, M., Rizzo, G., Savi, A., and Fazio, F. (1996). Registration of multi-modal biomedical images of the heart. *Q. J. Nucl. Med.*, 40(1):142–150.

Gilardi, M. C., Rizzo, G., Savi, A., Landoni, C., Bettinardi, V., Rossetti, C., Striano, G., and Fazio, F. N. (1998). Correlation of SPECT and PET cardiac images by a surface matching registration technique. *Computerized Medical Imaging and graphics*, 22:391–398.

Goerres, G. W., Kamel, E., Heidelber, T.-N. H., Schwitter, M. R., Burger, C., and von Schulthess, G. K. (2002). PET-CT image co-registration in the thorax: influence of respiration. *Eur. J. Nucl. Med.*, 29(3):351–360.

Habboosh, A. W. (1992). A review of MRI and PET correlation. In *Proc. IEEE Conf. in Bioengineering*, pages 16–17.

Hajnal, J., Hill, D., and Hawkes, D. (2001). *Medical image registration*. CRC Press.

Hämäläinen, M. and Nenonen, J. (1999). *Encyclopedia of Electrical Engineering*, volume 12, chapter Magnetic Source Imaging, pages 464–479. New York: Wiley & Sons.

Hänninen, H., Takala, P., Mäkijärvi, M., Montonen, J., Korhonen, P., Oikarinen, L., Simelius, K., Nenonen, J., Katila, T., and Toivonen, L. (2001). Recording locations in multichannel magneto-cardiography and body surface potential mapping sensitive for regional exercise-induced ischemia. *Basic Res. Cardiol.*, 96:405–414.

Hartiala, J. and Knuuti, J. (1995). Imaging of heart by MRI and PET. *Ann. Med.*, 27:35–45.

Herk, M. V. (2000). *Handbook of Medical Imaging: Processing and Analysis*, chapter Image registration using chamfer matching, pages 515–527. Academic Press.

Hill, D. and Hawkes, D. (2000). *Handbook of Medical Imaging: Processing and Analysis*, chapter Across-modality registration using intensity-based cost functions, pages 537–553. Academic Press.

Hill, D. L. G., Batchelor, P. G., Holden, M. H., and Hawkes, D. J. (2001). Medical image registration. *Physics in medicine and biology*, 46(1):1–45.

Hoh, C., Dahlbom, M., Harris, G., Choi, Y., Hawkins, R., Philps, M., and Maddahi, J. (1993). Automated iterative three-dimensional registration of positron emission tomography images. *J. Nucl. Med.*, 34(11):2009–2018.

Kerwin, W. (2000). *Handbook of Medical Imaging: Processing and Analysis*, chapter Image processing and analysis in tagged cardiac MRI, pages 375–391. Academic Press.

Kim, R., Aw, T., Bacharach, S., and Bonow, R. (1991). Correlation of cardiac MRI and PET images using lung cavities as landmarks. In *Proc. IEEE Conf. Computers in Cardiology*, pages 49–52.

Klein, G. J. and Huesman, R. H. (2002). Four-dimensional processing of deformable cardiac PET data. *Medical Image Analysis*, 6:29–46.

Klein, G. J., Reutter, B. W., and Huesman, R. H. (2002). Four-dimensional affine registration models for respiratory-gated PET. *IEEE Trans. Medical Imag.*, 48(3):756–760.

Kramer, E., Noz, M., Sanger, J., Megibow, A., and Maguire, G. (1989). CT-SPECT fusion to correlate radiolabeled monoclonal antibody uptake with abdominal CT findings. *Radiology*, 172(10):861–865.

Lauterbur, P. (1973). Image formation by induced local interactions: Examples employing nuclear magnetic resonance. *Nature*, 242:190–191.

Lester, H. and Arridge, S. (1998). A survey of hierarchical non-linear medical image registration. *Pattern recognition*, 32:129–149.

Levin, D., Pelizzari, C., Chen, G., Chen, C.-T., and Cooper, M. D. (1988). Retrospective geometric correlation of MR, CT, and PET images. *Radiology*, 169(3):817–823.

Lötjönen, J., Reissman, P.-J., Magnin, I. E., and Katila, T. (1999). Model extraction from magnetic resonance volume data using the deformable pyramid. *Med. Image Anal.*, 3(4):387–406.

Lötjönen, J., Reissman, P.-J., Magnin, I. E., Nenonen, J., and Katila, T. (1998). A triangulation method of an arbitrary point set for biomagnetic problems. *IEEE Trans. Magn.*, 34(4):2228–2233.

Maes, F., Collignon, A., Vandermeulen, D., Marchal, G., and Suetens, P. (1997). Multimodality image registration by maximization of mutual information. *IEEE Trans. Med. Imaging*, 16(2):187–198.

Maintz, J. B. A. and Viergever, M. A. (1998). A survey of medical image registration. *Med. Image Anal.*, 2(1):1–36.

Mäkelä, T., Pollari, M., Lötjönen, J., Pauna, N., Reilhac, A., Clarysse, P., Magnin, I. E., and Katila, T. (2003). Evaluation and comparison of surface and intensity based rigid registration methods for thorax and cardiac MR and PET images. In *Second International Workshop on Functional Imaging and Modeling of the Heart, FIMH 2003, accepted for publication*.

Mattes, D., Haynor, D., Vesselle, H., Lewellen, T., and Eubank, W. (2003). PET-CT image registration in the chest using free-form deformations. *IEEE Trans. Med. Imaging*, 22(1):120 –128.

Maurer, C. and Fizpatrick, J. M. (1993). A review of medical image registration. *Interactive image-guided neurosurgery*, pages 17–44.

McLeish, K., Hill, D., Atkinson, D., Blackall, J., and Razavi, R. (2003). A study of the motion and deformation of the heart due to respiration. *IEEE Trans. Med. Imaging*, 21(9):1142 –1150.

Montonen, J., Ahonen, A., Hämäläinen, M., Ilmoniemi, R., Laine, P., Nenonen, J., Paavola, M., K. Simelius, K., Paavola, M., Simola, K. S. J., and Katila, T. (2000). Magnetocardiographic functional imaging studies in biomag laboratory. In Aine, C., editor, *Biomag96, Proc. Tenth Internat. Conf. on Biomagnetism*, pages 494–497.

Nekolla, S., Ibrahim, T., Balbach, T., and Klein, C. (2000). *Understanding cardiac imaging techniques - from basic pathology to image fusion*, chapter Coregistration and fusion of cardiac magnetic resonance and positron emission tomography studies, pages 144–154. IOS Press, Amsterdam.

Nelder, J. and Mead, R. (1965). A simplex method for function minimization. *Comp. J.*, 7:308–313.

Nenonen, J. (1994). Solving the inverse problem in magnetocardiography. *IEEE Eng. Med. Biol.*, 13:487–496.

Nenonen, J., Pesola, K., Hänninen, H., K. Lauerma, K., Takala, P., Mäkelä, T. J., Mäkijärvi, M., Knuuti, J., Toivonen, L., and Katila, T. (2001). Current-density estimation of exercise-induced ischemia in patients with multivessel coronary artery disease. *Journal of Electrocardiography*, 34(suppl.):37–42.

Nenonen, J. T. (1997). Multimodal cardiac source imaging in the biomag laboratory. *Biomedizinische technik*, 42(1):29–32.

O'Connor, M. (2000). Evaluation of motion-correction techniques in cardiac SPECT. *J. Nucl. Med.*, 41(7):1298.

O'Connor, M., Kanal, K., Gebhard, M., and Rossman, P. (1998). Comparison of four motion correction techniques in SPECT imaging of the heart: a cardiac phantom study. *J. Nucl. Med.*, 39:2027–2034.

O'Dell, W. G., Moore, C. C., Hunter, W. C., Zerhouni, E. A., and McViegh, E. R. (1995). Three-dimensional myocardial defomations: calculation with displacement field fitting to tagged MR images. *Radiology*, 195:829–835.

Pallotta, S., Gilardi, M. C., Bettinardi, V., Rizzo, G., Landoni, C., Striano, G., Masi, R., and Fazio, F. (1995). Application of a surface matching image registration technique to the correlation of cardiac studies in positron emission tomography by transmission images. *Physics in Medicine and Biology*, 40:1695–1708.

Patton, J., Delbeke, D., and Sandler, M. (2000). Image fusion using an integrated, dual-head coincidence camera with X-ray tube-based attenuation maps. *J. Nucl. Med.*, 41(8):1364–1368.

Pauna, N., Croisille, P., Costes, N., Reilhac, A., Mäkelä, T., Cozar, O., Janier, M., and Clarysse, P. (2003). A strategy to quantitatively evaluate MRI/PET cardiac registration methods using a monte carlo simulator. In *Second International Workshop on Functional Imaging and Modeling of the Heart, FIMH 2003, accepted for publication.*

Pelizzari, C. A., Ghen, G. T. Y., Spelbring, D. R., Weichselbaum, R. R., and Chen, C. T. (1989). Accurate three-dimensional registration of CT, PET and/or MR images of the brain. *J Comput Assist Tomogr*, 13(1):20–26.

Pesola, K., Lötjönen, J., Nenonen, J., Magnin, I., Lauerma, K., Fenici, R., and Katila, T. (2000). The effect of geometry and topology differences in boundary element models on magnetocardiographic localization accuracy. *IEEE Trans. Biomedical Eng.*, 47(9):1237–1247.

Pesola, K., Nenonen, J., Fenici, R., Lötjönen, J., Mäkijärvi, M., Fenici, P., Korhonen, P., Lauerma, K., Valkonen, M., Toivonen, L., and Katila, T. (1999). Bio-electromagnetic localization of a pacing catheter in the heart. *Phys. Med. Biol*, 44:2565–2578.

Pham, Q. (2002). *Segmentation et mise en correspondance en imagerie cardiaque multimodale conduites par un modele anatomique bi-cavites du coeur.* PhD thesis, Institut National Polytechnique de Grenoble, France.

Pham, Q. C., Vincent, F., Clarysse, P., Croisille, P., and Magnin, I. E. (2001). A FEM-based deformable model for the 3-D segmentation and tracking of the heart in cardiac MRI. In *Image and Signal Processing and Analysis ISPA 2001*, pages 250–254.

Pluim, J., Maintz, J., and Viergever, M. (2000). Image registration by maximization of combined mutual information and gradient information. *IEEE Trans. Med. Imaging*, 19(8):809–814.

Polhemus (1993). *3SPACE ISOTRAK II User's Manual.* Polhemus Inc., Colchester, Vermont, U.S.A.

Powell, M. (1962). An iterative method of finding stationary values of a function of several variables. *Comp. J.*, 5:147–151.

Press, W. H., Teukolsky, S. A., Vetterling, W. T., and Flannery, B. P. (1992). *Numerical Recipes in C: The art of scientific computing 2nd Edition.* Cambridge Univ. Press, Cambridge.

Pretorius, P. H. ., Xia, W., Kinag, M. A., Tsui, B. M. W., Pan, T. S., and Villegas, B. J. (1997). Evaluation of right and left ventricular volume and ejection fraction using a mathematical cardiac torso phantom. *J. Nucl. Med.*, 38(10):1528–1535.

Raichura, N., Entwisle, J., Leverment, J., and Beardsmore, C. (2001). Breath-hold MRI in evaluating patients with pectus excavatum. *British Journal of Radiology*, 74(884):701–708.

Ratib, O. (2000). *Handbook of Medical Imaging: Processing and Analysis*, chapter Quantitative analysis of cardiac function, pages 359–374. Academic Press.

Reilhac, A., Gregoire, M.-C., Costes, N., Levanne, F., Pierre, C., Diou, A., and Pujol, J.-F. (2000). A PET monte carlo simulateur from numerica phantom: Validation against the EXACT ECAT HR+ scanner. In *Proc. IEEE Medical Imaging Conference*, pages 1527–1531.

Reilhac, A., Lartizien, C., Costes, N., Sans, S., Comtat, C., and Evans, A. (2002). Accounting for singes rates related phenomena in PET monte-carlo based simulations. In *IEEE Nuclear Sciences Symposium, accepted for publication.*

Roche, A., Pennec, X., Malandain, G., and Ayache, N. (1998). The correlation ratio as a new similarity measure for multimodal image registration. In Wells, W. M., Colchester, A., and Delp, S., editors, *Lecture Notes in Computer Science 1496: Medical Image Computing and Computer-Assisted Intervention, MICCAI98*, pages 1115–1124. Springer.

Roche, A., Pennec, X., Malandain, G., and Ayache, N. (2001). Rigid registration of 3-D ultrasound with MR images : A new approach combining intensity and gradient information. *IEEE Trans. Med. Imaging*, 20(10):1038–1049.

Rogers, W. J., Shapiro, E. P., Weiss, J. L., Buchalter, M. B., Rademakers, F. E., Weisfeldt, M. L., and Zerhouni, E. A. (1991). Quantification of and correction for left ventricular systolic long-axis shortening by magnetic resonance tissue tagging and slice isolation. *Circulation*, 84(2):721–731.

Rueckert, D., Sonoda, L., Hayes, C., Hill, D., Leach, M., and Hawkes, D. (1999). Nonrigid registration using free-form deformations: Application to breast MR images. *IEEE Trans. Med. Imaging*, 18(8):712–721.

Savi, A., Gilardi, M., Rizzo, G., Pepi, M., Landoni, C., Rossetti, C., Lucignani, G., Bartonelli, A., and Fazio, F. (1995). Spatial registration of echocardiographic and positron emission tomographic heart studies. *Eur. J. Nucl. Med.*, 22(3):243–247.

Shekhar, R. and Zagrodsky, V. (2002). Mutual information-based rigid and nonrigid registration of ultrasound volumes. *IEEE Trans. Med. Imaging*, 21(1):9–22.

Siemens (2001). *Applications guide, MAGNETOM Vision to MAGNETOM Sonata*, chapter Fast imaging with TurboFLASH, pages B.5.1–B.5.10. Siemens AG, Erlanger, Germany.

Siltanen, P. (1988). *Comprehensive Electrocardiology*, chapter Magnetocardiography. Oxford: Pergamon Press.

Simelius, K. (1998). Development of cardiographic mapping techniques for clinical use. *Licenciate thesis, Helsinki university of Technology.*

Sinha, S., Sinha, U., Czernin, J., Porenta, G., and Schelbert, H. (1995). Noninvasive assessment of myocardial perfusion and metabolism: feasibility of registering gated MR and PET images. *Am. J. Roentgenol.*, 36:301–307.

Slomka, P., Gilbert, A., Stephenson, J., and Cradduc, T. (1995). Automated alignment and sizing of myocardial stress and rest scans to three-dimensional normal templates using an image registration algorithm. *J. Nucl. Med.*, 36:1115–1122.

Slomka, P. J., Dey, D., Przetak, C., and Baum, R. (2000). Automated 3-D spatial integration of 18-F FDG wholebody PET with CT. *J. Nucl. Med.*, 41(6):59P.

Slomka, P. J., Dey, D., Przetak, C., and Baum, R. (2001a). Automated nonlinear 3-D registration of 18-F FDG wholebody PET with thoracic CT. *J. Nucl. Med.*, 42(5):11P.

Slomka, P. J., Radau, P., Hurwitz, G. A., and Dey, D. (2001b). Automated three-dimensional quantification of myocardiac perfusion and brain SPECT. *Computerized Medical Imaging and graphics*, (25):153–164.

Stone, C., McCormick, J., Gilland, D., Greer, K., Coleman, R., and Jaszczak, R. (1998). Effect of registration errors between transmission and emission scans on a SPECT system using sequential scanning. *J. Nucl. Med.*, 39(2):365–373.

Studholme, C., Hill, D. L., and Hawkes, D. J. (1997). Automated three-dimensional registration of magnetic resonance and positron emission tomography brain images by multiresolution optimasation of voxel mesures. *Medical Physics*, 24(1):25–35.

Studholme, C., Hill, D. L., and Hawkes, D. J. (1999). An overlap invariant entropy mesure of 3d medical image aligment. *Pattern Recognition*, 32:71–86.

Sweet, W. (1951). The use of nuclear disintegration in the diagnosis and treatment of brain tumor. *New England Journal of Medicine*, (247):875–878.

Tai, Y.-C., Lin, K., Hoh, C., Huang, S., and Hoffman, E. (1997). Utilization of 3-D elastic transformation in the registration of chest X-ray CT and whole body PET. *IEEE Trans. Nucl. Med*, 44(4):1606–1612.

Thirion, J.-P. (1995). Fast non-rigid matching of 3-D medical images. Research Report 2547, INRIA.

Thirion, J.-P. (2001). *Understanding cardiac imaging techniques - from basic pathology to image fusion*, chapter Perfusion and motion from gated SPECT, pages 84–93. IOS Press, Amsterdam.

Turkington, T., DeGrado, T., Hanson, M., and R.E.Coleman (1997). Alignment of dynamic cardiac PET images for correction of motion. *IEEE Trans. Nucl. Sci.*, 44(2):235–242.

van den Elsen, P., Pol, E.-J., and Viergever, M. (1993). Medical image matching - A review with classification. *IEEE Engineering in Medicine and Biology*, 12(2):16–39.

Waiter, G. D., Al-Mohammad, A., Norton, M. Y., Redpath, T. W., Welch, A., and Walton, S. (2000). Regional myocardial wall thickening assessed at rest by ECG gated (18)F- FDG positron emission tomography and by magnetic resonance imaging. *Heart*, 84:332–333.

Webb, S. (1995). *The Physics of Medical Imaging*. Academic Press.

Wells, W., Viola, P., Atsumi, H., Nakajima, S., and Kikinis, R. (1996). Multi-modal volume registration by maximization of mutual information. *Med. Image Anal.*, 1(1):35–51.

Wirth, M. A., Choi, C., and Jennings, A. (1997). Point-to-point registration of non-rigid medical images using local elastic transformation methods. In *IEEE Int. Conf. on Image Processing and its Applications*, pages 780–784.

Woods, R. (2000a). *Handbook of Medical Imaging: Processing and Analysis*, chapter Within-modality registration using intensity-based cost functions, pages 529–536. Academic Press.

Woods, R. (2000b). *Handbook of Medical Imaging: Processing and Analysis*, chapter Validation of registration accuracy, pages 491–497. Academic Press.

Wrenn, F. and Handlerp, M. P. (1951). The use of positron emitting radioisotopes for localization of brain tumors. *Science*, 113:153–164.

Yu, J. N., Fahey, F. H., Gage, H. D., Eades, C. G., Harkness, B. A., and Pelizzari, C. A. (1995). Intermodality, retrospective image registration in the thorax. *J. Nucl. Med.*, 36(12):2333–2338.

Zhenghong, L. and Berridge, M. (2002). PET imaging-based evaluation of aerosol drugs and their delivery devices: nasal and pulmonary studies. *IEEE Trans. Med. Imaging*, 21(10):1324–1331.